XI: $C_{10}H_{12}N_2O_2$; orthorhombic $P2_12_12_1$ space group; a = 13.762 (7) Å, b = 8.638 (4) Å, c = 7.907 (4) Å, Z = 4, R = 0.064, R_w = 0.084 for 965 significant reflections ($F_o > 0.0$) $\{w = 0.4684/[\sigma^2(F_o) + 0.0242F_o^2]\}$.

XII: $C_8H_{12}N_2O_2$; monoclinic $C2/c$ space group; a = 13.032 (6) Å, b = 8.776 (4) Å, c = 9.103 (5) Å, β = 128.74 (2)°, Z = 4, R = 0.062, R_w = 0.089 for 745 significant reflections ($F_o > 0.0$) $\{w = 1.0000/[\sigma^2(F_o) + 0.0686F_o^2]\}$.

XIII: $C_{10}H_{10}N_2O_2$; triclinic $P\bar{1}$ space group; a = 10.727 (5) Å, b = 8.219 (4) Å, c = 5.901 (3) Å, α = 103.22 (3), β = 100.85 (3), γ = 79.49 (3)°, Z = 2, R = 0.076, R_w = 0.108 for 1682 significant reflections ($F_o > 0.0$) $\{w = 0.4754/[\sigma^2(F_o) + 0.0305F_o^2]\}$.

Acknowledgment. The research was partially supported by Technion VPR Fund, Lawrence Deutsch Research Fund. S.F.N. and S.C.B. thank the National Foundation for partial financial support.

Registry No. I, 61195-22-0; II, 54168-24-0; III, 102494-19-9; IV, 102494-20-2; V, 102494-21-3; VII, 78790-57-5; VIII, 23292-39-9; IX, 72282-77-0; X, 77762-21-1; XI, 72282-78-1; XII, 3661-10-7; XIII, 23196-38-5; spiro[2.4]hepta-4,6-diene, 765-46-8; 4-methyl-1,2,4-triazoline-3,5-dione, 13274-43-6.

Supplementary Material Available: Listing of observed and calculated structure factors, atomic coordinates, and anisotropic temperature factors (129 pages). Ordering information is given on any current masthead page.

Mechanism of Ketone n → π* Optical Activity. Experimental and Computed Chiroptical Properties of 4-Axial and 4-Equatorial Alkyladamantan-2-ones[1]

David A. Lightner,*[2a] Thomas D. Bouman,*[2b] W. M. Donald Wijekoon,[2a] and Aage E. Hansen[2c]

Contribution from the Departments of Chemistry, University of Nevada, Reno, Nevada 89557-0020, and Southern Illinois University, Edwardsville, Illinois 62026-1652, and the Department of Physical Chemistry, H.C. Ørsted Institute, DK-2100 Copenhagen Ø, Denmark. *Received August 12, 1985*

Abstract: (1*S*,3*R*)-4*S*(a)- and 4*R*(e)-substituted adamantan-2-ones were prepared and their circular dichroism (CD) spectra measured. The substituent groups include methyl, ethyl, isopropyl, *tert*-butyl, neohexyl, and deuterio. The long-wavelength $n \rightarrow \pi^*$ CD transitions of the equatorial alkyladamantanones agree in sign and magnitude with octant rule predictions for *back* octants, while those of the axial isomers agree with predictions based upon front octants. The deuterio ketones exhibit the expected reversed-octant contributions of deuterium located in a back octant for each isomer. Calculations in the random phase approximation (RPA) are analyzed to determine the mechanisms responsible for the rotatory intensity. A μ–m mechanism is extracted from effective bond transition moments, and a set of additive bond increments is displayed that combines features of both the "perturbed chromophore" and "through-bond coupling" models for ketone optical activity. The mechanistic analysis shows octant-consignate coupling contributions, but the nature of the third nodal surface of the octant rule remains an a posteriori construct.

In the nearly 25 years since Moffitt et al.[3] proposed the octant rule for chiral saturated alkyl ketones, it has enjoyed wide application in interpreting details of absolute configuration and conformation from the circular dichroism (CD) or optical rotatory dispersion spectrum. The rule divides all space surrounding the carbonyl chromophore into eight regions (octants), and the octant occupied by a particular atom or group (perturber) determines the sign of its contribution to the rotatory strength of the $n \rightarrow \pi^*$ transition. The octants are derived, in part, from the local symmetry (C_{2v}) of the carbonyl group: reflection of a perturber across either of the symmetry planes *XZ* and *YZ* in Figure 1 leads to a mirror image molecular fragment and hence to an oppositely signed contribution to the rotatory strength. The quadrants thus defined are further divided into front and back octants by a third surface supposedly associated with the non-symmetry-determined nodes of the relevant carbonyl n and π^* orbitals.

As originally proposed, the third surface is a plane bisecting the C=O bond (Figure 1, left). More recently, the results from CNDO/S calculations were used to construct a concave third surface (Figure 1, right), in better agreement with experiment.[4-6] In practical applications the contributions from different substituents are assumed to be additive, and Figure 1, middle, shows the sign distribution defined as *consignate*[7] for rotatory strength contributions from alkyl perturbers in the respective octants. Atoms having counterparts symmetrically placed across the carbonyl symmetry planes (*XZ*, *YZ*) and atoms lying in symmetry planes are assumed to make no net contribution to the CD.

In this form the octant rule is simple and straightforward to apply, and has been used in establishing the absolute configuration of a large number of natural products or their derivatives and in

(1) The Octant Rule. 18. For part 17 see; Lightner, D. A.; Chang, T. C.; Hefelfinger, D. T.; Jackman, D. E.; Wijekoon, W. M. D.; Givens, J. W., III. *J. Am. Chem. Soc.* **1985**, *107*, 7499-7508.

(2) (a) University of Nevada, Reno. (b) Southern Illinois University, Edwardsville. (c) H. C. Ørsted Institute.

(3) Moffitt, W.; Woodward, R. B.; Moscowitz, A.; Klyne, W.; Djerassi, C. *J. Am. Chem. Soc.* **1961**, *83*, 4013-4018.

(4) Bouman, T. D.; Lightner, D. A. *J. Am. Chem. Soc.* **1976**, *98*, 3145-3154.

(5) (a) Lightner, D. A.; Chang, T. C. *J. Am. Chem. Soc.* **1974**, *96*, 3015-3016. (b) Lightner, D. A.; Jackman, D. E. *J. Chem. Soc., Chem. Commun.* **1974**, 344-345.

(6) (a) Snatzke, G.; Eckhardt, G. *Tetrahedron* **1968**, *24*, 4543-4558. (b) Snatzke, G.; Ehrig, B.; Klein, H. *Tetrahedron* **1969**, *25*, 5601-5609. (c) Lightner, D. A.; Jackman, D. E. *J. Am. Chem. Soc.* **1974**, *96*, 1938-1939.

(7) (a) Klyne, W.; Kirk, D. N. *Tetrahedron Lett.* **1973**, 1483-1486. (b) Kirk, D. N.; Klyne, W. *J. Chem. Soc., Perkin Trans. 1* **1974**, 1076-1103.

0002-7863/86/1508-4484$01.50/0

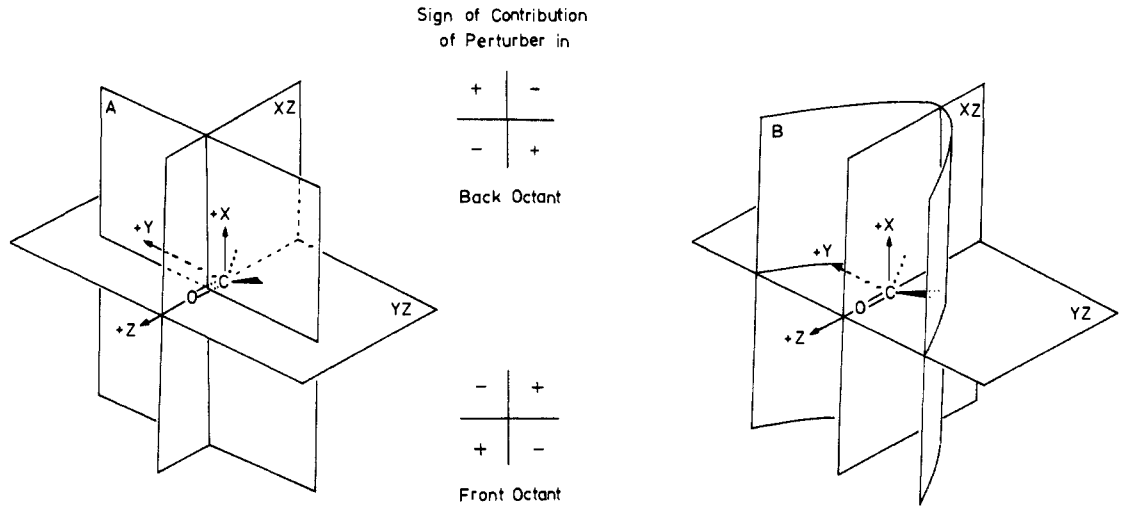

Figure 1. (Left) Classical octant rule diagram (ref 3) for the ketone carbonyl n → π* transition. Local symmetry-derived, orthogonal octant planes *XZ* and *YZ* divide all space into quadrants, and a non-symmetry-derived third nodal surface (A) is approximated by an orthogonal plane bisecting the C=O bond. "Front" octants are those nearer an observer along the +*z* axis, while "back" octants lie towards −*z*. (Middle) Octant contribution signs that perturbers make in back and front octants. (Right) Revised octant rule (ref 4) with octant planes *XZ* and *YZ* unchanged and the third nodal surface defined theoretically as a concave surface (**B**).

the conformational analysis of ketones whose absolute configuration had been determined independently.[8] However, despite widespread applications, there are still relatively few archetypical octant-rule molecules available,[8c,9] i.e., rigid-skeleton compounds whose dissymmetric perturbers probe into either back or front octants, and which become achiral when the substituents are replaced by hydrogen atoms. Availability of such compounds is of course important for the empirical evaluation of the range of validity of the octant rule.

On the theoretical side, an important goal is to provide insight into the mechanism behind chiroptical intensites, i.e., the way in which different parts of a molecule interact to generate the resulting sign and magnitude of the rotatory strength of a given transition. A general framework for the discussion of such mechanisms was provided by Kirkwood,[10] whose original formulation of optical rotatory power led to a distinction among three types of contributions, namely the one-electron (static perturbation) model, the electric dipole–magnetic dipole (μ–m) coupling, and the polarizability (μ–μ) theory. Again, despite a long history, the electronic mechanism behind the octant rule is still debated. The mechanism which was first suggested and studied computationally was that of a static chiral perturbation generated by partially screened nuclei,[11] and a μ–m mechanism was also suggested.[12] Later all-electron, whole-molecule calculations have attempted to extract atomic and/or bond contributions, without really relating such decompositions to a mechanism.[4,13-16] Perhaps the most striking result of these decompositions is the demonstration of the importance of electric dipole contributions from

Scheme I

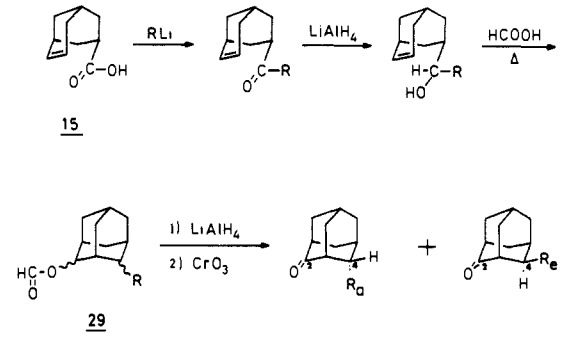

"open zigzag" lines,[4,14,15a] i.e., W-shaped bond patterns extending away from the carbonyl group (α-axial, β-equatorial, etc.).

The list of previous attempts at atom and bond decompositions includes some of our own work.[4,14,15a] However, we have recently developed a procedure by which the results of an all-electron calculation of rotatory and oscillator strengths can be analyzed into terms of the same form as the original Kirkwood contributions.[15b] This analysis, which involves no approximations beyond those entering the computational scheme for the overall excitation properties, was applied to the study of chiral monoolefins.[15b] For these systems we found that all three Kirkwood-type mechanisms contribute significantly for most transitions, with the polarizability contributions as the most important.

For a study of the octant rule, β-alkyladamantanones are particularly strong candidates for archetypical model compounds. Their skeleton is structurally rigid with a chair cyclohexanone moiety, the skeleton possesses C_{2v} molecular symmetry, which coincides with the local symmetry of the carbonyl chromophore,[14] and β-equatorial substituents definitely probe back octants whereas β-axial substituents can probe front octants. In this work, therefore, we describe the syntheses and circular dichroism spectra of a wide variety of monosubstituted β-axial and β-equatorial adamantanones. Included in the set of substituents are a number of different alkyl groups, and another type which has been demonstrated to show deviations from "normal" octant rule behavior, namely deuterium.[17] For several of the smaller alkyladamantanones, we apply our analysis scheme to results we obtain by ab initio calculations in the random phase approximation (RPA).[18-20] The RPA is a method designed to give linear response

(8) (a) Sing, Y. L.; Numan, H.; Wynberg, H.; Djerassi, C. *J. Am. Chem. Soc.* **1979**, *101*, 5155–5158; errata, *Ibid* **1979**, *101*, 7439. (b) Lee, S.-F.; Barth, G.; Djerassi, C. *J. Am. Chem. Soc.* **1981**, *103*, 295–301. (c) For leading references see Barth, G.; Djerassi, C. *Tetrahedron* **1981**, *37*, 4123–4142.

(9) (a) Djerassi, C. *Optical Rotatory Dispersion*; McGraw-Hill: New York, 1961. (b) Crabbe, P. *Optical Rotatory Dispersion and Circular Dichroism in Organic Chemistry*; Holden-Day: San Francisco, 1965. (c) Deutsche, C. W.; Lightner, D. A.; Woody, R. W.; Moscowitz, A. *Annu. Rev. Phys. Chem.* **1969**, *20*, 407–448. (d) Legrand, M.; Rougier, M. J. *Stereochemistry*; Kagan, H. B., Ed.; G.; Thieme: Stuttgart: 1977; Vol. 2, pp 33–183.

(10) Kirkwood, J. G. *J. Chem. Phys.* **1937**, *5*, 479; *7*, 139.

(11) Bouman, T. D.; Moscowitz, A. *J. Chem. Phys.* **1968**, *48*, 3115–3120.

(12) (a) Schellman, J. A. *J. Chem. Phys.* **1966**, *44*, 55–63. (b) Schellman, J. A. *Acc. Chem. Res.* **1968**, *1*, 144–151.

(13) Pao, Y. H.; Santry, D. P. *J. Am. Chem. Soc.* **1966**, *88*, 4157–4163.

(14) Lightner, D. A.; Bouman, T. D.; Wijekoon, W. M. D.; Hansen, Aa. E. *J. Am. Chem. Soc.* **1984**, *106*, 934–944.

(15) (a) Bouman, T. D.; Voigt, B.; Hansen, Aa. E. *J. Am. Chem. Soc.* **1979**, *101*, 550–558. (b) Hansen, Aa. E.; Bouman, T. D. *J. Am. Chem. Soc.* **1985**, *107*, 4828–4839.

(16) Howell, J. M. *J. Chem. Phys.* **1970**, *53*, 4152.

(17) Lightner, D. A.; Gawronski, J. K.; Bouman, T. D. *J. Am. Chem. Soc.* **1980**, *102*, 1983–1990.

(18) Hansen, Aa. E.; Bouman, T. D. *Adv. Chem. Phys.* **1980**, *44*, 545–644.

properties, such as excitation energies and transition moments, correct through first order in electron correlation.[20] We have found the method highly effective for the chiroptical properties of organic molecules.

In what follows we will describe the synthesis and stereochemistry of the substituted adamantanones, and then address the details of molecular geometry with the aid of molecular mechanics calculations and the CD spectra of the molecules considered. Following a brief presentation of the RPA method and the analysis scheme, we will examine the overall computed results. Next, we will discuss the mechanistic analysis of the computed intensities, and finally conclude with the relation to earlier work.

Synthesis and Stereochemistry

All of the substituted adamantanones (**1**–**14**) were prepared from (+)-*endo*-bicyclo[3.3.1]non-6-ene-3(*R*)-carboxylic acid (**15**),[21a,b] which was obtained from adamantan-2-one via (1) an

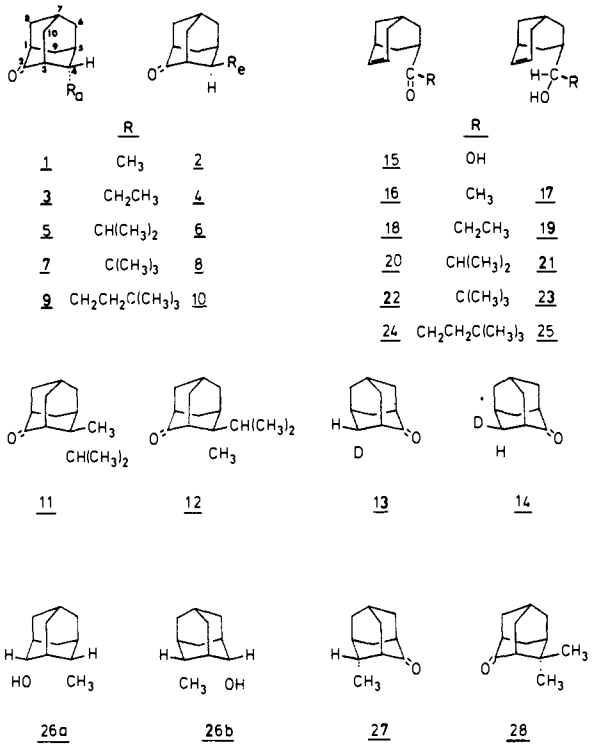

abnormal Schmidt reaction (using NaN_3/CH_3SO_3H) to give 4(e)-methanesulfonoxyadamantan-2-one, followed by (2) a quasi-Favorskii reaction (in KOH/aqueous ethanol) to give (+)-*endo*-bicyclo[3.3.1]non-6-ene-3-carboxylic acid,[22] and then (3) resolution by repeated crystallization of the dehydroabietylamine salt. Treatment of **15** with the appropriate alkyllithium reagent gave the corresponding bicyclo[3.2.1]non-6-en-3-yl ketones (Scheme I). This reaction worked smoothly to give the methyl (**17**), ethyl (**19**), isopropyl (**21**), and neohexyl (**25**) ketones, but with difficulty to give the more sterically hindered *tert*-butyl (**23**) ketone. Under the best conditions (refluxing pentane) the yield with *tert*-butyllithium was only 24%, but recovered starting acid (**16**) could be recycled. Reduction ($LiAlH_4$) of the ketones to the corresponding secondary alcohols followed by solvolysis (hot HCO_2H) re-formed the adamantane skeleton and led to a mixture of diastereomeric formates (**29**). Reduction of **29** followed by

Scheme II

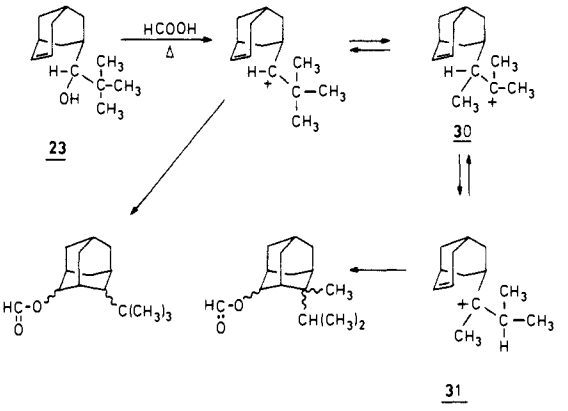

Jones oxidation yielded a mixture of epimeric 4(a)- and 4(e)-substituted adamantan-2-ones that could be separated by preparative gas chromatography, with the axial epimer being faster moving.

Only with the solvolyses of alcohol **23** did we encounter difficulties in re-forming the adamantane without rearrangement. With **23** (and **21**) we were concerned about possible Wagner–Meerwein rearrangements during solvolysis. In the isopropyl derivative, no rearranged product could be isolated; however, with the *tert*-butyl derivative (**24**), 1,2-methyl and hydrogen migrations (Scheme II) apparently occur to give significant amounts of rearranged carbocation **31**, which serves as the precursor to the major reaction products adamantanones **11** and **12**. The desired *tert*-butyladamantanones (**7** and **8**) can be recovered from the reaction, albeit in low yield, but homoadamantanones, e.g., from cyclization via carbocation **30** were not found. Formation of **7** and **8** gives the first symmetric chair cyclohexanones with β-*tert*-butyl groups in (1) an axial configuration and (2) an equatorial configuration.[23]

The enantiomeric excess (e.e.) of the adamantanones follows from that previously assigned to the carboxylic acid **15** by (1) ^{13}C NMR analysis of the derived 4,4-dimethyladamantan-2-one ketal with (*R*)-(−)-butane-2,3-diol[21c] and (2) by HPLC separation of the diastereomeric amides of **16** formed with (−)-α-phenylethylamine.[21a,b] The absolute configuration of acid **15** followed from application of the octant rule to the derived 4,4-dimethyladamantan-2-one[21a] (prepared by reacting **16** methyl ester with methyl Grignard followed by cyclization in hot formic acid, then hydrolysis and oxidation). Since our studies involve an analysis of the octant rule, we felt that we should confirm the absolute configuration by an independent method. We used the LIS–NMR analysis technique[24] on the Mosher esters[25] of the adamantanols derived from **1** and **5**. Thus, $LiAlH_4$ reduction of **1** reacted stereospecifically to give the syn alcohol (**26a** and/or **26b**). Similarly, **3** gave the corresponding syn isopropyl alcohol. Reaction of the alcohols with the acid chloride of (*R*)-(+)-α-methoxy-α-(trifluoromethyl)phenylacetic acid [(*R*)-(+)-MTPA][25] gave the corresponding Mosher esters. In the ^{19}F NMR spectra, the diastereomeric CF_3 signals of the Mosher esters were split into two lines, with the more intense signal at higher field. The integrated intensities gave the e.e. of the Mosher esters, hence the e.e. of the precursor adamantanones (and thus **15**), all in very good agreement with the values from the previous methods. Addition of $Eu(fod)_3$ caused a greater downfield shift ($\Delta\delta$) of the more shielded CF_3 resonance, corresponding to the (1*S*,3*R*) absolute configuration,[24] e.g., **26a** and **15**, again in agreement with the

(19) Jørgensen, P.; Simons, J. *Second Quantization-Based Methods in Quantum Chemistry*; Academic: New York, 1981.
(20) For a recent review, see Oddershede, J.; Jørgensen, P.; Yeager, D. L. *Comput. Phys. Rep.* **1984**, *2*, 33–92.
(21) (a) Numan, H.; Troostwijk, C. B.; Wieringa, J. H.; Wynberg, H. *Tetrahedron Lett.* **1977**, 1761–1764. (b) Numan, H.; Wynberg, H. *J. Org. Chem.* **1978**, *43*, 2232–2236. (c) Hiemstra, H.; Wynberg, H. *Tetrahedron Lett.* **1977**, 2183–2187.
(22) Sasaki, T.; Eguchi, S.; Toru, T. *J. Org. Chem.* **1970**, *35*, 4109–4114.
(23) Lightner, D. A.; Wijekoon, W. M. D. *J. Am. Chem. Soc.* **1985**, *107*, 2815–2817. β-Axial *tert*-butylcyclohexanone moieties have been reported previously in decalones (Goldsmith, D. J.; Thottathil, J. K. *J. Org. Chem.* **1982**, *47*, 1382–1384) with only minor distortion in the cyclohexanone ring. Goldsmith, D. J., personal communication.
(24) Kalyanam, N.; Lightner, D. A. *Tetrahedron Lett.* **1979**, 415–418.
(25) (a) Dale, J. A.; Dull, D. L.; Mosher, H. S. *J. Org. Chem.* **1969**, *34*, 2543–2549. (b) Dale, J. A.; Mosher, H. S. *J. Am. Chem. Soc.* **1973**, *95*, 512–519.

Scheme III

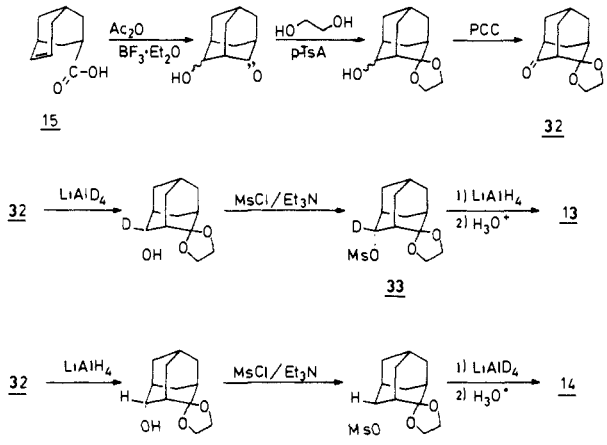

absolute configuration determined by application of the octant rule.[21a]

Deuterio ketones **13** and **14** were prepared by a modification of the method of Numan and Wynberg.[21b] Thus, as per Scheme III, carboxylic acid **15** was cyclized in acetic anhydride–boron trifluoride etherate to give a mixture of epimeric 4-hydroxyadamantan-2-ones, which was derivatized as the ethylene ketals and oxidized to ketone ketal **32**. Axial deuterioadamantanone **13** was prepared by reduction of **32** with $LiAlD_4$ followed by derivatization of the resulting hydroxy ketal as the methanesulfonate ester (**33**), then $LiAlH_4$ displacement of methanesulfonate with inversion of configuration. When the order of introduction of deuterium was reversed, first with $LiAlH_4$ reduction of **32** and then $LiAlD_4$ displacement of protio-**33**, the equatorial deuterioadamantanone (**14**) was obtained.

NMR and Mass Spectra

The ^{13}C NMR assignments are given in Table I and show in the deuterioadamantanones **13** and **14** the expected[26] small upfield shifts of the carbon (C-4) bearing the deuterium substituent. The differing effects of axial and equatorial substituents can be seen in, e.g., a slightly more deshielded C=O carbon in the axially substituted ketones and in the relative position of the substituent carbon attached to the ring: it is more deshielded in axial substituents than in equatorial. The expected large γ-gauche effects[27] are found at C-10 in the axial alkyladamantanones and at C-6 and C-9 in the equatorial isomers. Interestingly, the influence of the *tert*-butyl substituent on the γ-gauche ring carbon is much less pronounced than that of the other groups. The *tert*-butyl substituent also has a special effect on C-8: the axial *tert*-butyl leads to $\simeq$2 ppm deshielding relative to adamantanone, the equatorial to $\simeq$2 ppm shielding. As seen in the ^1H NMR, axial group hydrogens experience a shielding effect due to the proximal C=O group and resonate at slightly higher field than hydrogens of equatorial groups. This effect amounts to $\Delta\delta \simeq 0.14$ for the CH_3 groups of **1** (relative to **2**) and **7** (relative to **8**). The CH_3 groups of both **7** and **8** are equivalent at room temperature, suggesting rapid rotation about the bond connecting the *tert*-butyl groups to adamantanone. We estimate $\simeq$4.5 kcal/mol for the rotation barrier through an eclipsed conformation. The CH_3 groups of both isopropyl ketones **5** and **6**, however, each show two well-separated doublets for the diastereotopic methyls.

The high-resolution mass spectra of the adamantanones of this work show a prominent molecular ion peak, and variable, usually weak loss of H_2O peaks. There is an increasing tendency to cleave the substituent group from the adamantanone moiety as the substituent size increases (to give an m/z 149 peak). Interestingly, with the axial *tert*-butyladamantanone (**7**), the base peak is due to loss of m/z 56 (C_4H_8) rather than m/z 57, even at low ionizing

Table I. Carbon-13 NMR Assignments for Substituted Adamantanones[a]

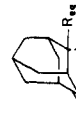

carbon	**13** D	**1** Me	**3** Et	**5** *i*-Pr	**7** *t*-Bu	**9** CH_2CH_2-*t*-Bu	**14** D	**2** Me	**4** Et	**6** *i*-Pr	**8** *t*-Bu	**10** CH_2CH_2-*t*-Bu
1	46.93 (d)	46.64 (d)	46.18 (d)	46.58 (d)	46.75 (d)	46.81 (d)	46.81 (d)	45.82 (d)	45.58 (d)	45.94 (d)	46.58 (d)	46.40 (d)
2	218.39 (s)	217.88 (s)	216.65 (s)	218.17 (s)	219.93 (s)	217.76 (s)	218.05 (s)	217.70 (s)	216.03 (s)	218.05 (s)	218.81 (s)	217.81 (s)
3	46.93 (d)	53.13 (d)	50.86 (d)	49.45 (d)	49.16 (d)	49.45 (d)	46.81 (d)	51.90 (d)	49.24 (d)	48.33 (d)	43.63 (d)	50.50 (d)
4	39.62	43.07 (d)	49.17 (d)	55.71 (d)	59.33 (d)	52.08 (d)	38.80 (d)	39.91 (d)	46.70 (d)	52.78 (d)	57.80 (d)	46.52 (d)
5	27.45 (d)	32.83 (d)	30.27 (d)	28.79 (d)	33.96 (d)	31.02 (d)	27.39 (d)	32.36 (d)	29.44 (d)	28.44 (d)	33.40 (t)	30.32 (d)
6	36.22 (t)	37.63 (t)	37.23 (t)	37.86 (t)	40.51 (t)	37.92 (t)	36.22 (t)	29.61 (t)	29.91 (t)	30.32 (t)	35.40 (t)	30.90 (t)
7	27.45 (d)	26.80 (d)	26.87 (d)	28.15 (d)	28.11 (d)	27.51 (d)	27.39 (d)	27.27 (d)	27.44 (d)	26.81 (d)	30.10 (d)	27.20 (d)
8	39.21 (t)	39.32 (t)	38.92 (t)	30.50 (t)	41.36 (t)	39.85 (t)	39.15 (t)	38.97 (t)	38.28 (t)	38.97 (t)	37.61 (t)	39.38 (t)
9	39.21 (t)	39.50 (t)	39.16 (t)	39.91 (t)	43.16 (t)	41.37 (t)	39.15 (t)	32.01 (t)	31.66 (t)	32.00 (t)	37.05 (t)	32.54 (t)
10	39.21 (t)	33.59 (t)	33.31 (t)	34.06 (t)	34.89 (t)	34.00 (t)	39.15 (t)	39.15 (t)	38.45 (t)	39.09 (t)	41.20 (t)	41.84 (t)
11		18.50 (q)	24.94 (t)	26.98 (d)	29.67 (s)	27.51 (t)		16.80 (q)	22.98 (t)	26.27 (d)	29.01 (s)	25.74 (t)
12			10.78 (q)	20.84 (q)	29.28 (q)	30.08 (t)			11.10 (q)	21.02 (q)	29.76 (q)	30.14 (t)
13				19.84 (q)	29.28 (q)	39.62 (s)				20.31 (q)	29.76 (q)	29.15 (s)
14					29.28 (q)	29.20 (q)					29.76 (q)	29.26 (q)
15						29.20 (q)						29.26 (q)
						29.20 (q)						29.26 (q)

[a] In $CDCl_3$ at 25.1 MHz, using a deuterium lock on δ 77.0; values in ppm downfield from tetramethylsilane.

(26) See, for example: Wherli, F. W.; Wirthlin, T. *Interpretation of Carbon-13 NMR Spectra*; Heyden: Philadelphia, 1978; pp 107–109.
(27) See, for example: Breitmaier, E. *^{13}C NMR Spectroscopy*; Verlag Chemie: New York, 1978; pp 74–75; and ref 25, pp 38 and 43.

Table II. Coordinates of Substituent Carbon Atoms in Selected 4(a)- and 4(e)-Alkyladamantan-2-ones and Total Steric Energy from MM2[a] Molecular Mechanics Energy-Minimized Geometries

ketone	substituent		coordinates, Å X	Y	Z	total steric energy, kcal/mol
1	(a) CH_3		2.54334	1.46656	−0.90471	19.802
2	(e) CH_3		1.50531	2.56932	−2.46963	20.326
3	(a) CH_2CH_3	CH_2	2.53542	1.48721	−0.87920	21.263
		CH_3	3.82886	1.55544	−1.70225	
4	(e) CH_2CH_3	CH_2	1.49925	2.61037	−2.43837	21.843
		CH_3	2.86049	2.72509	−3.13958	
5	(a) $CH(CH_3)_2$	CH	2.57088	1.49448	−0.88807	23.389
		CH_3	2.62130	2.88692	−0.22614	
		CH_3	3.84998	1.31959	−1.72950	
6	(e) $CH(CH_3)_2$	CH	1.52095	2.61395	−2.47824	23.908
		CH_3	2.87125	2.61830	−3.22256	
		CH_3	1.47519	3.84736	−1.55465	
7	(a) $C(CH_3)_3$	C	2.56950	1.69986	−1.21585	28.473
		CH_3	3.74308	1.31633	−2.14471	
		CH_3	2.86163	1.12194	+0.18487	
		CH_3	2.60195	3.24469	−1.06993	
8	(e) $C(CH_3)_3$	C	1.82227	2.59586	−2.29800	30.176
		CH_3	3.35744	2.49149	−2.50306	
		CH_3	1.58244	3.77622	−1.32848	
		CH_3	1.22362	2.98523	−3.66366	

[a] Limited certainty in values begins with the fourth significant figure (ref 29).

Table III. Reduced Rotatory Strengths[a] of (1S,3R)-4-Equatorial Alkyladamantan-2-ones and (1R,3S)-4(e)-Deuterioadamantan-2-one

compd	substituent	solvent	$[R]^{25}$	$[R]^{0}$	$[R]^{-50}$	$[R]^{-100}$	$[R]^{-150}$	$[R]^{-175}$
2	CH_3	EPA[b]	2.097	2.208	2.214	2.129	2.101	2.077
		MI[c]	1.537	1.767	1.786	1.825	1.830	1.847
		EPA-MI[d]	0.560	0.441	0.428	0.304	0.271	0.230
4	CH_2CH_3	EPA	2.355	2.362	2.232	2.230	2.171	2.177
		MI	2.398	2.367	2.333	2.318	2.242	2.258
		EPA-MI	−0.043	−0.005	−0.101	−0.088	−0.071	−0.081
6	$CH(CH_3)_2$	EPA	2.509	2.501	2.368	2.235	2.152	2.135
		MI	1.412	1.460	1.378	1.299	1.230	1.210
		EPA-MI	1.097	1.041	0.990	0.936	0.922	0.925
8	$C(CH_3)_3$	EPA	2.255	2.227	2.118	2.037	1.932	1.986
		MI	1.482	1.493	1.485	1.996	1.956	2.010
		EPA-MI	0.773	0.734	0.633	0.041	−0.024	−0.024
10	$CH_2CH_2C(CH_3)_3$	EPA	3.169	3.142	2.991	2.906	2.771	2.773
		MI	2.096	2.112	2.043	2.030	2.034	2.093
		EPA-MI	1.073	1.037	0.948	0.876	0.677	0.680
14	D	EPA	0.272	0.275	0.243	0.260	0.250	0.249
		MI	0.341	0.337	0.324	0.305	0.281	0.278
		EPA-MI	−0.069	−0.062	−0.081	−0.045	−0.031	−0.029

[a] $[R]$ is rotatory strength (cgs units), $\times 1.08 \times 10^{40}$. Values are corrected to 100% e.e. and for solvent contraction. The superscript numbers are temperatures, ±2, in °C. [b] EPA = diethyl ether–isopentane–ethanol, 5:5:2 (v/v/v). [c] MI = methylcyclohexane–isopentane, 4:1 (v/v). [d] Difference values, $[R]_{EPA}^{T} - [R]_{MI}^{T}$.

voltages. We interpret this unusual and unexpected major fragmentation to represent one of the extremely few cases of a ketone homo-McLafferty rearrangement.[28] In all cases, there is a prominent fragment ion due to loss of (substituent + CO) at m/z 121.

Molecular Geometry and Circular Dichroism

Because the adamantanone skeleton is itself symmetric, the axial and equatorial substituents of **1–12** may be viewed as the elements controlling the sign and magnitude of the n → π* Cotton effect (CE) according to the octant rule. In order to determine the exact octant locations of the alkyl substituents we used MM2 molecular mechanics calculations,[29] and as Table II shows, there is, as expected, little variation in the location of the substituent carbon attached to the ring, and all alkyl substituents prefer a staggered conformation, as viewed from this carbon to C-4 of the adamantanone. For the staggered conformation of the *tert*-butyl group, however, one CH_3 must lie in a sterically hindered position over a ring—either the cyclohexanone (in **7**) or the cyclohexane (in **8**). Its eclipsed rotamer is ≃5 kcal/mol higher in conformational energy. The CH_3 groups of ethyl (**3**, **4**) and isopropyl (**5**, **6**) prefer to face away from the ring rather than over it by ≃3.5 kcal/mol. Among these staggered conformers available to the ethyl group, there is only ≃0.23 kcal/mol energy difference between the + synclinal and antiperiplanar rotamers (CH_3/C-3 reference). The locations of the substituents will be useful in an analysis of the circular dichroism (CD) spectra.

The CD spectra of equatorially substituted adamantanones are given in Figures 2 and 3. All of the equatorial substituents lie well behind the carbonyl carbon in an upper left (or lower right) *back* octant and are thus each expected to make a (+) octant contribution to the CD CE. The CE magnitudes, as measured by their reduced rotatory strengths $[R]$, are largely temperature-invariant down to −175 °C (Table III) in both polar (EPA) and hydrocarbon (MI) solvents. Thus, there are no large conformational changes as a function of temperature, see e.g., ethyl (**4**) and neohexyl (**10**). Solvent effects, as measured by $[R]_{EPA} - [R]_{MI}$, are most prominent with isopropyl (**6**) and neohexyl (**10**) adamantanones, perhaps reflecting greater solvent-dependent octant orientations of these substituents. Taking note of the nearly identical $[R]$ values in EPA for methyl, ethyl, isopropyl, and *tert*-butyl, it would appear that the major net contribution of the

(28) Kingston, D. G. I.; Bursey, J. T.; Bursey, M. M. *Chem. Rev.* **1974**, *74*, 215–242.
(29) Allinger, N. L.; Yuh, Y. Y. *QCPE 423* (adapted for CDC by S. Profeta), Quantum Chemistry Program Exchange, Indiana University, Bloomington, IN.

Table IV. Reduced Rotatory Strengths[a] of (1*S*,3*R*)-4(a)-Alkyladamantan-2-ones and (1*R*,3*S*)-4(a)-Deuterioadamantan-2-one

compd	substituent	solvent	$[R]^{25}$	$[R]^{0}$	$[R]^{-50}$	$[R]^{-100}$	$[R]^{-150}$	$[R]^{-175}$
1	CH_3	EPA[b]	−0.100	−0.120	−0.262	−0.492	−0.862	−0.916
		MI[c]	+0.0784	−0.095	−0.305	−0.436	−0.671	−0.758
		EPA − MI[d]	−0.178	−0.025	+0.043	−0.056	−0.191	−0.158
3	CH_2CH_3	EPA	−0.362	−0.375	−0.450	−0.652	−0.786	−0.880
		MI	−0.200	−0.252	−0.293	−0.404	−0.748	−0.950
		EPA − MI	−0.162	−0.123	−0.157	−0.221	−0.038	+0.070
5	$CH(CH_3)_2$	EPA	−0.453	−0.462	−0.522	−0.637	−0.905	−0.969
		MI	−0.320	−0.354	−0.383	−0.590	−0.792	−0.901
		EPA − MI	+0.133	+0.108	+0.139	+0.047	−0.113	−0.062
7	$C(CH_3)_3$	EPA	−1.670	−1.709	−1.663	−1.752	−1.696	−1.703
		MI	−0.978	−0.980	−0.948	−0.905	−0.880	−0.907
		EPA − MI	−0.692	−0.729	−0.715	−0.847	−0.816	−0.796
9	$CH_2CH_2C(CH_3)_3$	EPA	−0.580	−0.571	−0.678	−0.768	−0.917	−1.072
		MI	−0.300	−0.302	−0.363	−0.598	−0.862	−1.248
		EPA − MI	−0.280	−0.269	−0.315	−0.017	−0.055	+0.176
13	D	EPA	0.021	0.022	0.020	0.020	0.021	0.022
		MI	0.039	0.041	0.041	0.042	0.039	0.037
		EPA − MI	−0.018	−0.019	−0.021	−0.022	−0.018	−0.015

[a] $[R]$ is rotatory strength (cgs units), × 1.08 × 10^{40}. Values are corrected to 100% e.e. and for solvent contraction. The superscript numbers are temperatures, ±2, in °C. [b] EPA = diethyl ether–isopentane–ethanol, 5:5:2 (v/v/v). [c] MI = methylcyclohexane–isopentane, 4:1 (v/v). [d] Difference values, $[R]_{EPA}^{T} - [R]_{MI}^{T}$.

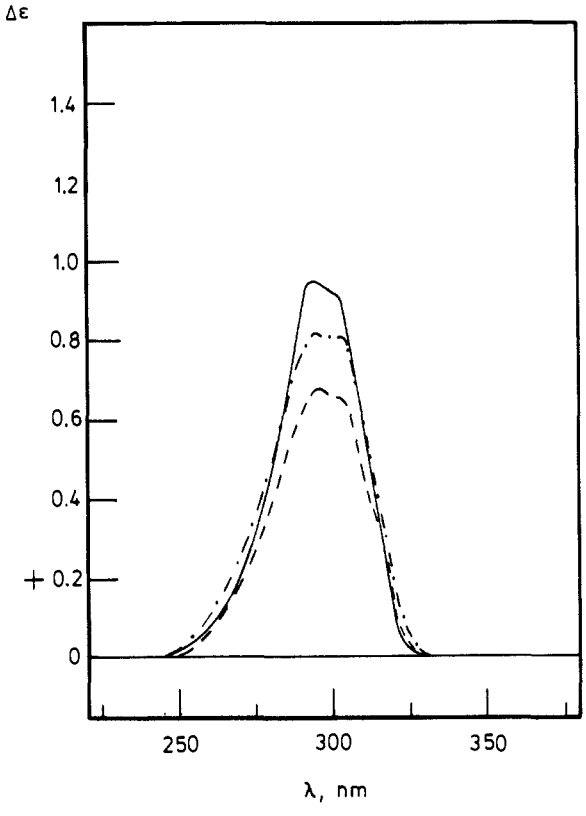

Figure 2. Circular dichroism spectra of 10^{-3} M (1*S*,3*R*)-4(e)-substituted adamantan-2-ones in EPA (ether–isopentane–ethanol, 5:5:2, v/v/v) run at 25 °C and corrected to 100% e.e. The equatorial substituents are (2) methyl (- - - - -), $\Delta\epsilon_{295}^{max} = +0.67$; (4) ethyl (– · – · –), $\Delta\epsilon_{295}^{max} = +0.81$; (6) isopropyl (approximately – · – · –), $\Delta\epsilon_{295}^{max} = +0.80$; (8) *tert*-butyl (approximately – · – · –), $\Delta\epsilon_{295}^{max} = +0.771$; (10) neohexyl (—), $\Delta\epsilon_{295}^{max} = +0.92$.

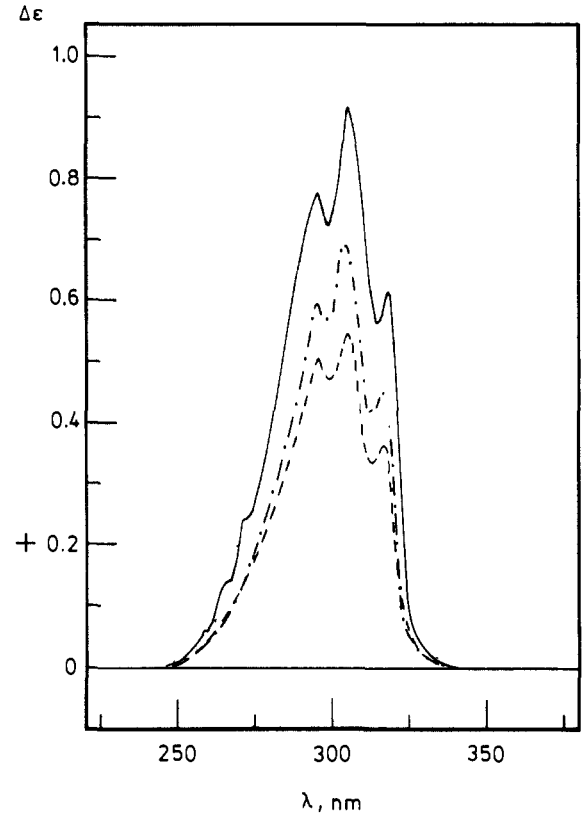

Figure 3. Circular dichroism spectra of 10^{-3} M (1*S*,3*R*)-4(e)-substituted adamantan-2-ones in MI (methylcyclohexane–isopentane, 4:1, v/v) run at 25 °C and corrected to 100% e.e. The equatorial substituents are (2) methyl (- - - - -), $\Delta\epsilon_{305}^{max} = +0.54$; (4) ethyl (—), $\Delta\epsilon_{306}^{max} = +0.91$; (6) isopropyl (approximately · · · · ·), $\Delta\epsilon_{306}^{max} = +0.60$; (8) *tert*-butyl (approximately · · · · · ·), $\Delta\epsilon_{305}^{max} = +0.75$; (10) neohexyl (· · · · · ·), $\Delta\epsilon_{306}^{max} = +0.69$.

first substituent carbon attached to the ring controls the sign and magnitude of the CE, with its appended CH_3's either providing cancelling contributions or making only weak ones. The deuterioadamantanone (**14**) shows the previously recognized reversed octant contribution of the deuterium perturber due to the effective C–D bond length decrease.[17,21b,30]

The β-axial position of cyclohexanone, e.g. as represented in 4(a)-substituted adamantan-2-ones, was first thought to project into a back octant[3] and later considered to be an antioctant site.[8a,b,9c,13] More recently, a β-axial CH_3 perturber has been viewed as lying in a *front* octant, very near to the third nodal surface.[5] The axially substituted adamantanones of this work therefore serve as models to explore front octants, since perturbers larger than CH_3 may project well into a front octant. For the absolute configuration shown for **1**–**12**, if the perturbers lie in an upper left front octant, they will be expected to make (−) contributions to the CD CE; indeed as Figures 4 and 5 show, the CEs are all strongly negative, except for the CH_3 perturber in **1**, where the CE in hydrocarbon solvent is weakly (+) at 25 °C. At low

(30) Lightner, D. A.; Chang, T. C.; Horwitz, J. *Tetrahedron Lett.* **1977**, 3019–3020; erratum. *Ibid* **1978**, 696.

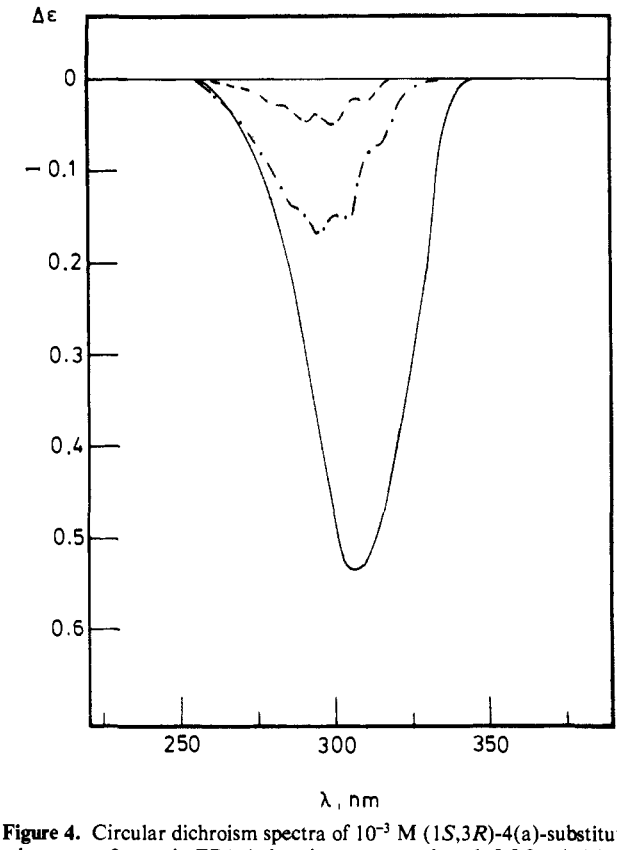

Figure 4. Circular dichroism spectra of 10^{-3} M (1*S*,3*R*)-4(a)-substituted adamantan-2-ones in EPA (ether–isopentane–ethanol, 5:5:2, v/v/v) run at 25 °C and corrected to 100% e.e. The axial substituents are (1) methyl (- - - - -), $\Delta\epsilon_{306}^{max} = -0.046$; (3) ethyl (approximately · · · · · ·), $\Delta\epsilon_{296}^{max} = -0.15$; (5) isopropyl (- · - · -), $\Delta\epsilon_{297}^{max} = -0.17$; (7) *tert*-butyl (—), $\Delta\epsilon_{296}^{max} = -0.54$; (9) neohexyl (· · · · · ·), $\Delta\epsilon_{296}^{max} = -0.17$.

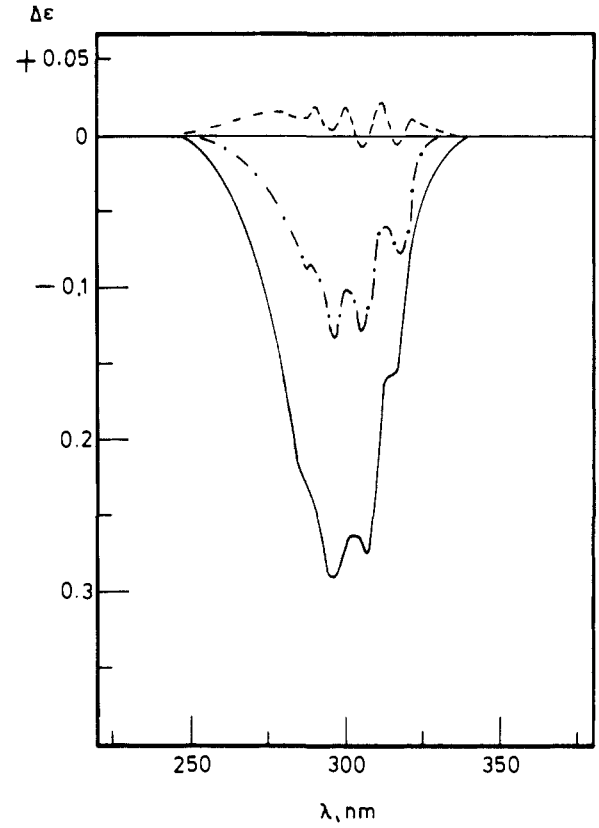

Figure 5. Circular dichroism spectra of 10^{-3} M (1*S*,3*R*)-4(a)-substituted adamantan-2-ones in MI (methylcyclohexane–isopentane, 4:1, v/v) run at 25 °C and corrected to 100% e.e. The axial substituents are (1) methyl (- - - - -), $\Delta\epsilon_{313}^{max} = +0.025$; (3) ethyl (approximately · · · · · ·), $\Delta\epsilon_{301}^{max} = -0.10$; (5) isopropyl (- · - · -), $\Delta\epsilon_{297}^{max} = -0.15$; (7) *tert*-butyl (—), $\Delta\epsilon_{296}^{max} = -0.29$; (9) neohexyl (approximately · · · · · ·), $\Delta\epsilon_{297}^{max} = -0.10$.

temperatures, the [*R*]s are uniformly strongly negative, even for **1** (Table IV). The pronounced temperature and solvent effects in the CD of **1**, whose β-axial CH_3 perturber lies close to a nodal surface, have been ascribed previously to the importance of restricted rotation and solvent perturbation of the C=O chromophore or vibronic effects. Larger perturbers do not show such a pronounced temperature sensitivity, but the trend is generally toward larger [*R*] values at −175 °C than at 25 °C. In fact, the [*R*] values at −175 °C are essentially the same for all alkyl substituents. This result is surprising and suggests again that the substituent carbon attached to the adamantanone framework acts in effect as the major contributor to the CE. The main exception to this observation is the case of **7** in EPA. In agreement with previous results,[21b] the β-axial deuterium (of **13**) makes a reversed-octant contribution, if one assumes that it lies in a back octant (in contrast with the β-axial alkyl perturbers), i.e., just behind the third nodal surface.[17]

Theory and Analysis

The rotatory strength R_{0q} for a transition from the ground state $|0\rangle$ to an excited state $|q\rangle$ can be given by the dipole velocity expression (in atomic units)[18]

$$R_{0q}^{\nabla} = (2c\Delta E_{0q})^{-1}\langle 0|\nabla|q\rangle\cdot\langle 0|r \times \nabla|q\rangle \qquad (1)$$

where ΔE_{0q} is the excitation energy, and where $\langle 0|\nabla|q\rangle$ and $\langle 0|r \times \nabla|q\rangle$ are respectively the electric and magnetic dipole transition moment vectors. Other expressions are available, but lend themselves less readily to the subsequent analysis.

The transition moments and excitation energies in eq 1 are computed in the random phase approximation (RPA),[19,20] which is discussed extensively elsewhere;[18,31,32] here we present only the relations needed to define our notation. In a basis of occupied (ϕ_a, ϕ_b...) and virtual Hartree–Fock molecular orbitals (ϕ_m, ϕ_n...), the RPA prescription for a transition moment of a Hermitian one-electron operator (such as **r**) may be written

$$\langle 0|r|q\rangle = 2^{1/2}\sum_a\sum_m\langle\phi_a|r|\phi_m\rangle S_{am,q} \qquad (2)$$

While the relevant anti-Hermitian one-electron operators yield

$$\langle 0|\nabla|q\rangle = 2^{1/2}\sum_a\sum_m\langle\phi_a|\nabla|\phi_m\rangle T_{am,q} \qquad (3a)$$

$$\langle 0|r \times \nabla|q\rangle = 2^{1/2}\sum_a\sum_m\langle\phi_a|r \times \nabla|\phi_m\rangle T_{am,q} \qquad (3b)$$

The coefficients $S_{am,q}$ and $T_{am,q}$, together with the excitation energies ΔE_{0q}, are determined from the coupled sets of linear RPA equations

$$\sum_{am}(\mathbf{A} + \mathbf{B})_{bn,am}S_{am,q} = \Delta E_{0q}T_{bn,q} \qquad (4a)$$

$$\sum_{am}(\mathbf{A} - \mathbf{B})_{bn,am}T_{am,q} = \Delta E_{0q}S_{bn,q'} \qquad (4b)$$

where **A** is a matrix containing the interactions between singly excited configurations (a → m) and (b → n), and **B** contains the interactions between the Hartree–Fock ground state and doubly excited configurations (a → m,b → n). The matrix elements can thus be labeled by indices referring only to singly excited configurations, as in eq 4, but the **B** matrix in fact introduces electron correlation. Setting the **B** matrix elements to zero makes $S_{am,q} = T_{am,q}$ and the problem reduces to conventional monoexcited CI. The (generally small) differences between the *S* and *T* coefficients turn out to be crucial for an adequate description of oscillator and rotatory strengths.

Analysis of Intensities. Assuming now that the occupied orbitals ϕ_a, ϕ_b ... have been localized, we define an excitation-characteristic

(31) Hansen, Aa. E.; Bouman, T. D. *Mol. Phys.* **1979**, *37*, 1713–1724.
(32) Bouman, T. D.; Hansen, Aa. E.; Voigt, B.; Rettrup, S. *Int. J. Quantum Chem.* **1983**, *23*, 595–611.

"bond" (bond or lone pair) electric dipole transition moment from eq 3a by summing over all the virtual orbitals:

$$\nabla_{a,q} = 2^{1/2}\sum_m \langle\phi_a|\nabla|\phi_m\rangle T_{am,q} \quad (5)$$

with a similar definition for the magnetic dipole transition moment, eq 3b.

$$\mathbf{l}_{a,q} = 2^{1/2}\sum_m \langle\phi_a|\mathbf{r} \times \nabla|\phi_m\rangle T_{am,q} \quad (6)$$

Expanding $\mathbf{l}_{a,q}$ relative to ρ_a, the centroid position of orbital ϕ_a,

$$\mathbf{l}_{a,q} = 2^{1/2}\sum_m \langle\phi_a|(\mathbf{r} - \rho_a) \times \nabla|\phi_m\rangle T_{am,q} + \rho_a \times \nabla_{a,q} \quad (7)$$

$$\equiv \mathbf{l}'_{a,q} + \rho_a \times \nabla_{a,q} \quad (8)$$

we obtain $\mathbf{l}'_{a,q}$ as an inherent bond magnetic dipole transition moment, while $\rho_a \times \nabla_{a,q}$ is a "moment of momentum" term. Substituting eq 2–7 into eq 1 yields

$$R_{0q} = \sum_a\sum_b R^q_{ab} = \sum_a\sum_b \{R^q(\mu_a,m_b) + R^q(\mu_b,m_a) + R^q(\mu_a,\mu_b)\} \quad (9)$$

where

$$R^q(\mu_a,m_b) = (4c\Delta E_{0q})^{-1}\nabla_{a,q}\cdot\mathbf{l}'_{b,q} \quad (9a)$$

$$R^q(\mu_b,m_a) = (4c\Delta E_{0q})^{-1}\nabla_{b,q}\cdot\mathbf{l}'_{a,q} \quad (9b)$$

$$R^q(\mu_a,\mu_b) = (4c\Delta E_{0q})^{-1}(\rho_a - \rho_b)\cdot(\nabla_{a,q} \times \nabla_{b,q}) \quad (9c)$$

A diagonal term (a = b) represents the "one-electron", or static perturbation mechanism, while the off-diagonal terms $R(\mu_a,m_b)$ and $R(\mu_b,m_a)$ in eq 9a and 9b represent two physically distinct electric dipole–magnetic dipole (μ–m) terms.[12] Equation 9c corresponds to the μ–μ, or polarizability term of Kirkwood.[10] Each term is origin-independent and so can be assigned a physical meaning, in contrast to earlier decompositions where separation of electric and magnetic dipole contributions was not possible.[14,16] The analysis applies as long as the transition moments can be written in the form of eq 3 regardless of how the coefficients $T_{am,q}$ are computed, and no approximations are introduced beyond those entering that computation. In the present formalism, all references to individual virtual orbitals have disappeared, so that the entire intensity can be discussed in terms of structural features (i.e., "bonds" or "lone pairs" ϕ_a, ϕ_b).

A static perturbation, or "one-electron", mechanism[11] would be reflected in terms $R(\mu_a, m_a)$ involving the orbitals associated with an isolated carbonyl chromophore, that is, the two oxygen lone pairs, the C=O double bond orbitals, and (perhaps) the remaining two σ bonds from the carbonyl carbon. The μ–m mechanism,[12] on the other hand, is expected to manifest itself through large $R(\mu_a,m_b)$ terms, where ϕ_b is a lone-pair orbital on oxygen. $R(\mu_a,\mu_b)$ terms would couple pairs of local electric dipole bond transition moments in a chiral manner.

While this analysis will yield a complete mechanistic picture of the couplings responsible for the overall optical activity, the picture may well be too detailed to be useful, especially if a large fraction of the $n_{occ}(n_{occ} + 1)/2$ bond pair contributions are similar in magnitude. A somewhat coarser grained picture can be obtained by condensing all contributions involving a particular orbital ϕ_a into one term:

$$R_{0q} = \sum_a [R^q_{aa} + \tfrac{1}{2}\sum'_b (R^q_{ab} + R^q_{ba})] \equiv \sum_a R^q_{a,eff} \quad (10)$$

where the q again is a reminder that these terms are specific to a particular excitation. These effective, gross bond contributions can be displayed on a structural diagram, and exhibit the net effect of a given bond on the total rotatory intensity, *in the presence of the rest of the molecule.*

Relation to Sector Rules. To demonstrate the relation of this analysis to sector rules, we consider two enantiomeric molecules arranged to be interrelated by a mirror operation in the *YZ* plane of a Cartesian master coordinate system. Pairing the labels so that the mirror operation takes bond orbital a in one enantiomer into a′ in the other, we notice that freedom of phase choice for the orbitals and the transformation properties of the operators allow the identifications

$$\{\nabla^x_{a,q}; \nabla^y_{a,q}; \nabla^z_{a,q}\} = \{-\nabla^x_{a',q}; \nabla^y_{a',q}; \nabla^z_{a',q}\} \quad (11a)$$

$$\{\rho^x_a; \rho^y_a; \rho^z_a\} = \{-\rho^x_{a'}; \rho^y_{a'}; \rho^z_{a'}\} \quad (11b)$$

$$\{l^x_{a,q}; l^y_{a,q}; l^z_{a,q}\} = \{l^x_{a',q}; -l^y_{a',q}; -l^z_{a',q}\} \quad (12)$$

reflecting the polar and axial vector transformations of the quantities in eq 11 and 12, respectively. Inspection of eq 9 then immediately demonstrates the expected pairing of oppositely signed bond contributions from two enantiomers. If in addition one enantiomer can be generated from the other by moving one or more perturbers across a symmetry plane of a parent skeleton molecule, then the above pairing of oppositely signed contributions amounts to the demonstration of a sector rule relative to a symmetry-determined surface. Such a symmetry-determined sector rule is clearly not excitation-specific, and for ketones, this consideration generates a quadrant rule.[12] On the other hand, there is no a priori basis for the prediction of the third surface, since such an excitation-specific sector rule will depend on a balance among the various terms in eq 9, each of which carries its own excitation-dependent sector behavior.

Computations and Results

We chose the two 4-methyladamantan-2-ones (**1** and **2**), the 4(a)-ethyl derivative (**3**) in two of its rotamers, and (4,4)-dimethyladamantanone (**28**) for computation and analysis of rotatory intensities. SCF molecular orbitals were generated using a modified version of GAUSSIAN 80.[33] Calculations on the monoalkyl derivatives were done on two geometries: the idealized cyclohexanone structure used previously, and the structure resulting from the MM2 calculations. The small differences in the two structures led to SCF energies that differ by about 6 kcal/mol, with the MM2 structure (somewhat surprisingly) lying *higher* than the idealized one. An energy uncertainty of this magnitude, even in determining conformational preference, seems to be characteristic of comparisons among results from SCF, MM2, and SCF corrected by second-order Møller–Plesset perturbation theory (MP2).[34]

As with our thioketone work,[14] the size of the adamantanones necessitated using only a minimal, STO-4G atomic orbital basis; our earlier results indicated that this basis set yielded satisfactory results for the n → π* excitation,[14] even though most other types of excitation are not well described. The SCF energies for the antiperiplanar and +synclinal conformations of **3** are virtually the same, so that we are unable to distinguish a clear conformational preference. This similarity persists even when the SCF energies are corrected for electron correlation (MP2).[34] All singly excited configurations arising from the valence occupied MO's were included in the RPA calculations; the largest such set included 1224 singly-excited configurations, and hence indirectly ca. 375 000 doubly-excited configurations. For purposes of analysis, the occupied MO's were localized using the Foster–Boys criterion,[15a] and the resulting "banana" double bonds in the C=O group were retransformed to recover local σ and π bonds.[15a] The virtual orbitals were not localized, since the summation over m in eq 5–7 makes it immaterial whether the virtual orbitals are localized or not.

The computed n → π* excitation energies and rotatory strengths for the chosen compounds are shown in Table V, for both geometries where appropriate. The experimental trends are reproduced correctly, but in the case of the MM2 structures, the shift in rotatory strength in going from equatorial to axial is not sufficient to change the sign. The idealized geometry results are in consistently better agreement with experiment, and are quite reasonable in view of the small basis set we have used.

(33) Van Kampen, P. N.; de Leeuw, F. A. A. M.; Smits, G. F.; Altona, C.; *QCPE 437*, Quantum Chemistry Program Exchange, Indiana University, Bloomington, IN, **1982**; Pople, J. A. et al. *QCPE 406*, **1981**.
(34) Binkley, J. S.; Pople, J. A. *Int. J. Quantum Chem.* **1975**, *9*, 229–236.
(35) Murray, R. K., Jr.; Goff, D. L. *J. Org. Chem.* **1978**, *43*, 3844–3848.

Table V. Comparison of Computed and Observed Chiroptical Properties of the n → π* Excitation in **1–3** and **28**

compd	calcd idealized λ_{max}[a]	calcd idealized $[R^{\nabla}]$	calcd MM2 λ_{max}	calcd MM2 $[R^{\nabla}]$	exptl[b] λ_{max}	exptl[b] $[R]^{-175}$
4(e)-CH_3 (**2**)	289	1.24	284	1.03	295	1.96
4(a)-CH_3 (**1**)	289	−0.38	285	0.08	306	−0.84
4(a)-C_2H_5 (**3**) + sc	288	−0.31	284	0.09	296	−0.92
4(a)-C_2H_5 (**3**)ap	289	−0.28	284	0.18		
4,4-di-CH_3 (**28**)	289	0.85	–	–	303[c]	1.7[c]

[a] Wavelength in nm. [b] Average of values in EPA and MI. [c] Estimated from ref 21a for $\Delta\epsilon^{max}$ = +0.61 at 25 °C.

Table VI. Major Coupling Types Computed for Generating n → π* Optical Activity[a]

type	bond a	bond b	mechanism
1	C_α–C_β	$O(\pi_y)$	μ_a–m_b[b]
2	C_β–$H_{\beta\text{-eq}}$	$O(\pi_y)$	μ_a–m_b
3	C_α–C_β	C_2–$C_{\alpha'}$	~60% μ_a–m_b + ~40% μ_a–μ_b
4	C_β–$H_{\beta\text{-eq}}$	C_2–$C_{\alpha'}$	~55% μ_a–m_b + ~45% μ_a–μ_b
5	C_α–C_β	C_2–C_α	μ_a–m_b

[a] See Figure 6 for skeletal position labels. C_2 is the carbonyl carbon, and $O(\pi_y)$ is the in-plane π-type oxygen lone-pair orbital. [b] Greater than 90% a single type.

Table VII. Values of Computed Coupling Terms 1–5 (Reduced Rotatory Strength Units) in Each Quadrant for Molecules **1–3**, in the Idealized Geometry

molecule	type[a]	quadrant[b] I	II	III	IV
2	1	5.65	−5.45	−5.50	5.42
	2	3.28	−3.02	−2.96	2.97
	3	3.19	−3.06	−3.11	3.06
	4	1.97	−1.83	−1.79	1.79
	5	0.77	−0.73	−0.75	0.72
1	1	5.56	−5.39	−5.44	5.40
	2	2.64	−3.01	−2.94	3.00
	3	3.11	−3.02	−3.03	3.03
	4	1.61	−1.83	−1.76	1.81
	5	0.75	−0.71	−0.72	0.72
3 (+ sc)	1	5.56	−5.41	−5.45	5.44
	2	2.62	−3.00	−2.93	3.00
	3	3.12	−3.06	−3.07	3.07
	4	1.61	−1.83	−1.76	1.81
	5	0.76	−0.73	−0.73	0.75
3 (ap)	1	5.58	−5.45	−5.46	5.44
	2	2.60	−3.00	−2.93	3.00
	3	3.12	−3.07	−3.06	3.06
	4	1.59	−1.81	−1.75	1.81
	5	0.76	−0.73	−0.73	0.73

[a] See Table VI. [b] See Figure 6.

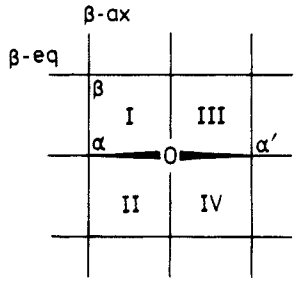

Figure 6. Octant projection diagram[3] for adamantanone showing numbering for quadrants determined by C_{2v} symmetry planes, and skeletal position nomenclature referred to in Table VII.

Figure 6 shows the quadrant projection of the adamantanone skeleton and our notation for quadrants and skeletal positions. In Table VI, we list the major coupling terms of the form of eq 9, in descending order of importance, and indicate the corresponding mechanistic type. Electric dipole couplings with the magnetic dipole moment of the oxygen "π_y" lone pair component

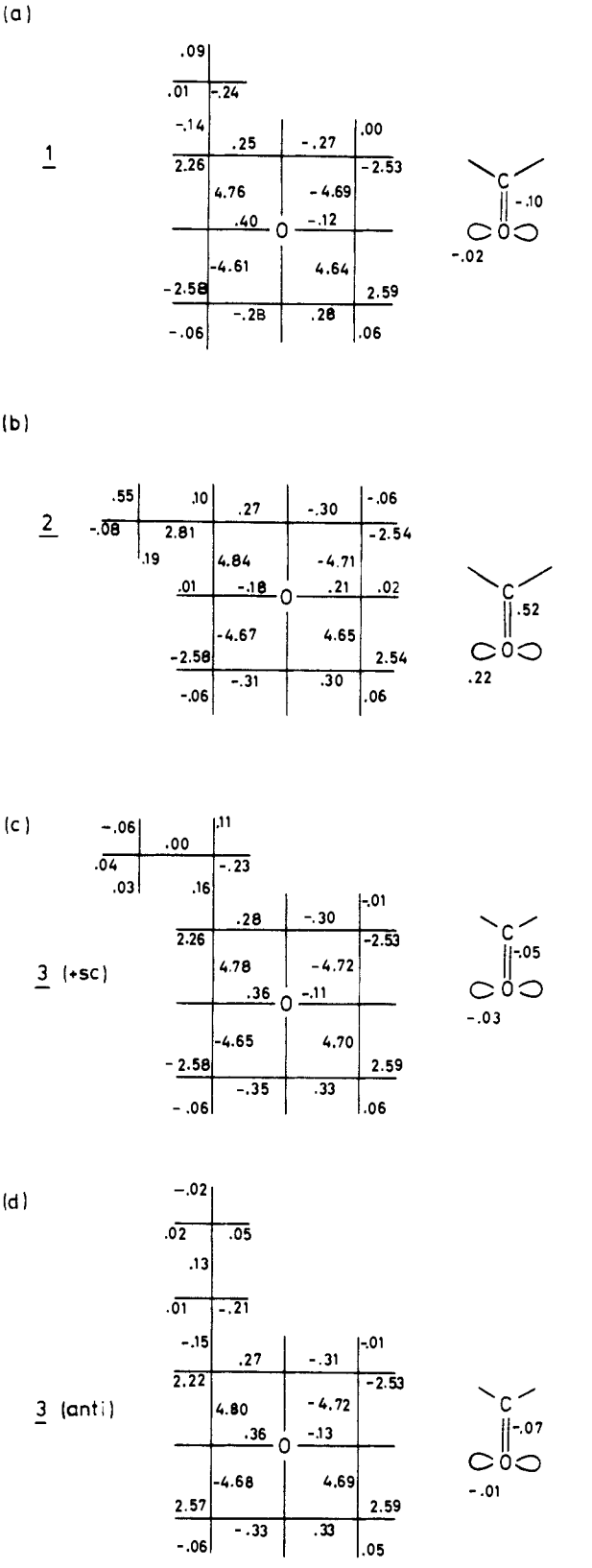

Figure 7. Computed effective bond contributions to $[R^{\nabla}]$, eq 10, displayed on octant projections, with carbonyl group contributions shown at right: (a) 4(a)-methyladamantan-2-one (**1**); (b) 4(e)-methyladamantan-2-one (**2**); (c) +synclinal rotamer of 4(a)-ethyladamantan-2-one (**3**); (d) antiperiplanar rotamer of **3**.

are numerically the largest. Table VII lists the values of these terms for each quadrant in the molecules computed. Overall, in terms of the mechanistic contributions in eq 9, about 79% of the total rotatory intensity comes from off-diagonal μ–m terms, eq 9a and 9b, while 15% comes from μ–μ couplings, eq 9c. The diagonal μ–m, or "one-electron" terms, eq 9a + 9b, contribute

Table VIII. Comparison of Observed and Estimated[a] Reduced Rotatory Strengths[b] of Isomeric 4-Isopropyl-4-methyladamantan-2-ones

compd	solvent	$[R]^{25}$	$[R]^{0}$	$[R]^{-50}$	$[R]^{-100}$	$[R]^{-150}$	$[R]^{-175}$
11	EPA[c]–obsd	2.217	2.140	2.064	2.101	2.106	2.038
	EPA–estd	1.644	1.746	1.692	1.492	1.196	1.108
	MI[d]–obsd	2.602	2.549	2.501	2.478	2.328	2.310
	MI–estd	1.217	1.413	1.403	1.235	1.038	0.946
12	EPA–obsd	1.640	1.632	1.617	1.623	1.637	1.618
	EPA–estd	2.409	2.381	2.106	1.743	1.290	1.219
	MI–obsd	2.017	2.006	1.986	1.978	1.834	1.831
	MI–estd	1.490	1.365	1.073	0.863	0.559	0.452

[a] Estimated by adding $[R]^T$ for isopropyl and $[R]^T$ for methyl as obtained from Tables III and IV. [b] EPA = diethyl ether–isopentane–ethanol, 5:5:2 (v/v/v). [c] MI = methylcyclohexane–isopentane, 4:1 (v/v). [d] Difference values, $[R]_{EPA}{}^T - [R]_{MI}{}^T$.

very little, 6%, although their signs are the same as those of the overall rotatory strength in **1–3**.

Figure 7 shows a condensation of the above fine-grained analysis according to eq 10, where all contributions involving a given orbital ϕ_a have been collapsed to a single term. Notice that all the larger bond contributions are consignate with the octant rule prescription for the respective octants. Since the effective bond contributions sum to the net rotatory strength for the molecule, these numbers can be compared approximately with the increment $\delta\Delta\epsilon$ values derived by Kirk and Klyne.[7b] It should be emphasized, however, that both the R_a^{eff} terms (eq 10) and the $\delta\Delta\epsilon$ values are only approximately independent of their surroundings, and a given term, e.g., C_α–C_β, may be perturbed significantly by other structural features that vary in a class of molecules.

Discussion

The Octant Rule and Surfaces. Table VII and Figure 7 show not only which couplings or bond contributions are large, but also that there are a number of nontrivial symmetry breaking (chiral) contributions from pairs of bonds which are related by the erstwhile symmetry of the skeleton. In fact these symmetry-breaking skeleton contributions are at least as important as direct contributions from the perturber, in marked contrast to the assumptions of the original octant rule.

For the surfaces we note that reflection of, say Figure 7a, in the vertical symmetry plane of the skeleton would give the mirror image of the numerical value of all bond contributions, and change all signs at the same time. This therefore represents a quadrant rule effect, albeit one that includes skeleton contributions, as discussed above and also in more general terms in connection with eq 11 and 12. The experimental CEs are consistent with the picture (Figure 1, right) of a concave third nodal surface that cuts behind the carbonyl carbon and extends outward toward oxygen,[4] but as discussed previously, the relation of the various coupling terms to this picture is not easily apparent. Some couplings involving the β-substituent do change sign between axial and equatorial forms, but other changes within the skeleton are also significant. It might be tempting to relate the sign changes computed for an axial substituent in the idealized vs. the MM2 geometries to a shift of the third nodal surface. It turns out, though, that these sign changes are *not* due to changed couplings on the axial methyl, but rather to small changes throughout the skeleton.

Figure 8 shows a plot of the transition density of the n → π^* excitation of **1**, in a plane 1 au above the plane of the C=O group. The dissymmetry of the transition density is not apparent on this scale, a fact which is also reflected in the computed oscillator strength of $<10^{-4}$. Since the transition density determines the electric dipole transition moment, an overall quadrant rule distribution is apparent from the density. The nodes of the n and π^* orbitals do not yield a single third nodal surface, but rather introduce only narrow regions of sign change. The third surface thus remains an a posteriori construction derived from the overall rotatory strengths, and no simple rationale is apparent at this time.

Additivity. The isomeric 4-isopropyl-4-methyladamantanones (**11** and **12**) allow an experimental test of the additivity of the octant contributions of isopropyl and methyl (Tables III and IV). The experimentally determined [R] values for **11** and **12** are shown in Table VIII along with the resulting estimated (additive) values.

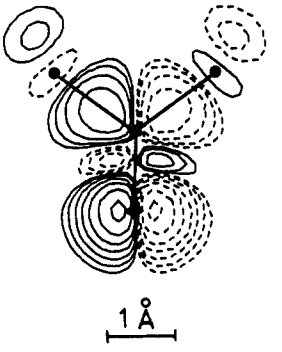

Figure 8. Transition density[15b] for n → π^* excitation of **1**, 1.0 atomic unit (0.53 Å) above ($x > 0$) the *YZ* plane. Successive contours differ by a factor of 2. The carbonyl group skeleton is superimposed for clarity. Solid and dashed contours indicate regions of (arbitrary) positive and negative phase, respectively.

It is interesting that the order of magnitude and CE sign are predicted correctly, but the numerical agreement between the estimated and observed values is not particularly good. It should be noted, however, that for these systems deviation from additivity can arise not only from nonadditive electronic effects, but also because the addition of a methyl group to C-4 of the isopropyl ketones **5** and **6** generates two new gauche CH_3/CH_3 interactions for what was previously the most stable rotamer of the isopropyl group. These new destabilizing interactions will tend to raise the importance of CE contributions from previously negligible conformers.

We were not able to make a direct comparison between the results for **11** and **12** above and computed RPA values, because of the size of these molecules. Instead, we computed n → π^* chiroptical properties for 4,4-dimethyladamantan-2-one (**28**), for which experimental CD results have been reported elsewhere.[21a] Table V compares these results with computed and experimental results for the two monomethyl compounds **1** and **2**. The latter are seen to be only roughly additive, whereas the computed results show additivity to a greater extent. The dependence of coupling contributions from the skeleton on the site and nature of alkyl substitution shows also that strict additivity is not to be expected.

Mechanism. Our analysis shows that dynamical μ–*m* coupling contributions dominate the resulting ketone n → π^* optical activity, and that the most important of these involve couplings between the localized nonbonding oxygen orbital and a zigzag pattern of bonds extending away from the carbonyl group. Static perturbation (one-electron) contributions play a very small role, while the overall polarizability contributions (μ–μ couplings) are small but not quite negligible. In fact, individual μ–μ terms can be large, but occur in nearly cancelling sets, showing that the chiral perturbations of the skeleton contributions are much larger for the μ–m terms than for the μ–μ terms.

Relation to Previous Work. In our earlier work on the octant rule, we wrote the electric dipole transition moment, eq 3a, as a sum of one- and two-center atomic orbital contributions and determined the importance of a zigzag pattern of bonds extending away from the carbonyl group.[4,15a] The magnetic dipole transition moment was not similarly analyzed, because of the origin dependence of such terms. However, in our more recent work on

the thio analogues of the methyladamantanones studied here,[14] we presented a decomposition of the rotatory strength at the atomic orbital level, leading to individually origin-invariant atom and bond coupling terms $R_{AB,CD}$, labeled by atomic indices, and we identified a number of leading coupling types.

The present analysis and our previous decompositions of octant rule effects share some similarities but also lead to differences in interpretation. The similarities include the importance of contributions from bonds along a zigzag line away from the chromophore, and the fact that a nontrivial part of the total rotatory strength comes from symmetry-breaking skeleton contributions. The principal difference is of course that the present analysis allows the extraction of Kirkwood-type mechanisms in terms of bond contributions. The price paid for this is the loss of the type of information about the relative importance of local and charge-transfer excitations which is contained in the $R_{AB,CD}$ atom and bond decomposition.

In more detail, we find that the present analysis makes the leading bond contributions consignate, whereas the $R_{AB,CD}$ decomposition makes some analogous contributions dissignate. This difference arises in part because of redistribution of terms and in part because the bond moments in eq 5–7 sample the entire molecule through the sum over all virtual orbitals, whereas an $R_{AB,CD}$ term samples atomic orbitals on the pertinent atoms only. The advantage of the present analysis is not only that it provides a well-defined decomposition into mechanistically as well as structurally meaningful contributions, but also that it is applicable to computations in extended as well as minimal basis sets; the $R_{AB,CD}$ decomposition is really applicable with impunity only in minimal basis set calculations.

Concluding Remarks

We have shown experimentally that the chiroptical properties of the n → π* transition of 4(e)-substituted adamantan-2-ones follow the octant rule for back octants, except for the previously recognized reversed-octant effect of deuterium. 4(a)-Substituted adamantan-2-ones follow the octant rule for front octants, consistent with our previous theoretically derived picture of the octant rule that locates the third nodal surface as concave and cutting behind the carbonyl carbon (Figure 1, right).[4] From the analysis described here, however, our current picture of the mechanism of ketone optical activity is primarily one of μ–m couplings controlled by W-shaped paths extending from the carbonyl group but with net bond contributions that obey the octant rule for perturbing groups. This detailed analysis does not seem to yield a picture of a third nodal surface in any simple way. We do find it gratifying, though, that the Kirkwood analysis yields a clear distinction between the mechanisms for optical activity in ketones and in olefins.[15b]

Experimental Section

General. Circular dichroism (CD) spectra were recorded on a JASCO J-40 instrument equipped with a photoelastic modulator and a J-DPY data processor, and a spectroscopic Dewar for variable-temperature CD measurements. Ultraviolet (UV) spectra were recorded on a Cary 219 or Beckman 25 spectrophotometer, and rotations were determined in 95% ethanol, unless otherwise indicated, on a Perkin-Elmer 141 polarimeter. All nuclear magnetic resonance (NMR) spectra were determined in $CDCl_3$ and reported in parts per million (δ) downfield from tetramethylsilane unless otherwise indicated on a JEOL FX-100 instrument. Mass spectra (MS) were recorded at 70- or 14-eV ionizing voltage on an Kratos MS-50 mass spectrometer at the Midwest Center for Mass Spectrometry, University of Nebraska. Infrared (IR) spectra were measured on a Perkin-Elmer Model 599 instrument. All melting points are uncorrected and were determined on a Thomas-Hoover or Mel-Temp capillary apparatus. Combustion analyses were performed by Micro-Analytical Lab, Mountain View, CA, or MicAnal, Tucson, AZ. Analytical gas chromatography (GC) was performed on a Varian-Aerograph Model 2400 F/I instrument on 6 ft × $^1/_8$ in. diameter columns with the indicated stationary phases that were adsorbed on 80/100 Chromosorb W-AW-DMCS: column A (20% FFAP), column **B** (5% SE-30) and column C (12% QF-1). Preparative gas chromatography (GC) was performed on 6 ft × $^3/_8$ in. diameter columns: column D (20% FFAP on 60/80 Chromosorb W-AW-DMCS) or column E (15% QF-1 on 70/80 Chromosorb W) using a Varian-Aerograph model 1720 T/C instrument. Spectral data were obtained using spectral grade solvents (MCB): methylcyclohexane–isopentane, 4:1 v/v (MI), ethyl ether–isopentane–ethanol, 5:5:2, v/v/v (EPA), and *n*-heptane. Other solvents were distilled and dried before use: benzene, pentane, chloroform, and dichloromethane from P_2O_5, acetone from $KMnO_4$, and diethyl ether from $LiAlH_4$ under N_2. The solvents were used freshly distilled or stored over 4-A molecular sieves (Linde). The $LiAlD_4$ used in this work was 99.8% from Alfa-Ventron. Column chromatography was accomplished on (0.05–0.20 mm) J. T. Baker silica gel.

***endo*-Bicyclo[3.3.1]non-6-ene-3-carboxylic Acid (15).** Sodium azide (10.8 g, 160 mmol) was added during 30 min to a mechanically stirred mixture of adamantan-2-one (Aldrich) (16.0 g, 107 mmol) in 98% methanesulfonic acid (Aldrich) (240 mL) at 2–5 °C. (**N.B.** Unless the methanesulfonic acid is relatively anhydrous, the reaction fails.) After 2 h of stirring at 20 °C, the mixture was poured onto ice, and the resulting mixture was made alkaline by adding 50% aqueous NaOH. After stirring for an additional 2 h at room temperature, the solution was extracted with ether (3 × 150 mL), and the aqueous solution containing the sodium salt of the acid was acidified with 35% HCl. The precipitate formed was extracted with ether (3 × 50 mL), and the ether extracts were washed with water (3 × 100 mL), dried (anhydrous Na_2SO_4), and evaporated to give white flakes of the desired carboxylic acid, 14.1 g (79.4%), mp 194–196 °C [lit.[22] mp 193–196 °C]. Continuous ether extraction of the combined aqueous solutions yielded an additional 1.1 g of acid.

Resolution of *endo*-Bicyclo[3.3.1]non-6-ene-3-Carboxylic Acid (15).[12a,b] Racemic acid (13.0 g, 78.3 mmol) and (+)-dehydroabietylamine {$[\alpha]_D$ +56.1° (*c* 2.4, pyridine), Aldrich} (22.36 g, 78.4 mmol) were heated at reflux together for 2 h in 95% ethanol (290 mL). The solution was cooled to room temperature slowly, and the precipitated salt was recrystallized 8 times to afford salt with $[\alpha]^{25}_{578}$ +75.81° (*c* 0.24). Crystallization of various combined fractions led to salts with intermediate rotations. Decomposition of the salt was achieved by shaking it with 10% aqueous HCl followed by ether extraction. The ether solution was back extracted with 2 N NaOH, and the combined alkaline extracts were acidified and extracted with ether. The ether was evaporated following drying (anhydrous Na_2SO_4) to afford crystalline acid. Salt with $[\alpha]^{25}_{578}$ +75.81° gave acid with $[\alpha]^{25}_{578}$ +112.4° (*c* 0.25); salt with $[\alpha]^{25}_{578}$ +5.77° gave acid with $[\alpha]^{25}_{578}$ −60.55° (*c* 0.23). The positively rotating acid has been shown to correspond to the absolute configuration represented by **15**, and its enantiomeric excess (e.e.) and absolute configuration are determined in the present work by NMR studies of the Mosher ester of its derivative (**26**).

(+)-(1*S*,5*R*)-*endo*-(3(*R*)-Bicyclo[3.3.1]non-6-enyl) Methyl Ketone (16). Exactly 1 g (6.02 mmol) of (+)-*endo*-bicyclo[3.3.1]non-6-ene-3-(*R*)-carboxylic acid (**15a**), $[\alpha]^{25}_{578}$ +79.61° (*c* 1.0), 52.97% e.e., was dissolved in dry ethyl ether and converted to its lithium salt by the addition of 50 mg of finely powdered LiH. The mixture was stirred at room temperature for 1 h, and then the solvent was removed by rotary evaporation. The resulting lithium salt was dried under vacuum at 80 °C. The dried salt (1.04 g) in 25 mL of dry ether was stirred vigorously while an ethereal solution of methyllithium (1.52 M, 5.0 mL, 7.6 mmol) was added to it at 0 °C. The mixture was stirred for 0.5 h at 0 °C after final addition and then for 3 h at room temperature, after which it was quenched by the addition of saturated aqueous NH_4Cl. The aqueous layer was separated and extracted with (3 × 25 mL) ether. The combined ether layers were washed with water (25 mL) and then 5% aqueous $NaHCO_3$ and dried ($MgSO_4$). Evaporation of the ether gave a pale yellow oil which was distilled (kugelrohr, 78 °C, 2 mm) [lit.[34] bp 70–73 °C, 0.5 mm] to give 0.86 g (87%) of the colorless, semisolid ketone **16**. It was >99% pure by GC on column A and had $[\alpha]^{25}_{589}$ +67.8°, $[\alpha]^{25}_{578}$ +71.24° (*c* 1.3); IR (neat) 3040, 2900, 1710, 1350 cm^{-1}; ^1H NMR δ 1.2–2.5 (br m, 11 H), 2.0 (s, 3 H, CH_3), 5.2–5.7 (m, 2 H, =CH).

(+)-(1*R*,5*S*)-*endo*-3(*R*)-(1-Hydroxyethyl)bicyclo[3.3.1]non-6-ene (17). Ketone **16** from above (0.77 g, 4.69 mmol) in 20 mL of dry ether was added dropwise to stirred slurry of $LiAlH_4$ (0.25 g) in ether (20 mL). The mixture was cooled and added to 50 mL of a 1:1 mixture of water–10% aqueous H_2SO_4. The aqueous layer was separated and extracted with ether (3 × 25 mL). The combined ether layers were washed with water (25 mL) and then 5% aqueous $NaHCO_3$ and dried ($MgSO_4$). After removal of the solvent by rotary evaporation and kugelrohr (94 °C, 2.5 mm) distillation, 0.70 g (90%) of alcohol **17** was obtained. It was >99% pure by GC on column A and had $[\alpha]^{25}_{589}$ +115.7°, $[\alpha]^{25}_{578}$ +121.8° (*c* 0.99); IR (neat) 3600–3200, 3025, 1050 cm^{-1}; ^1H NMR δ 0.9–2.05 (br m, 11 H), 1.0 (d, 3 H, *J* = 6 Hz, CH_3), 3.47 (br 1 H, OH), 5.5–5.9 (br t, 2 H, =CH) ppm.

Anal. Calcd for $C_{11}H_{18}O$ (166): C, 79.46; H, 10.91. Found: C, 79.20; H, 10.77.

(±)-(1*S*,3*R*)-4(*S*)(a)-Methyladamantan-2-one (1). Alcohol **17** (0.63 g, 3.79 mmol) from above was heated in formic acid (88%, 18 mL) at

100 °C. After heating 4 h, the solution was cooled, poured into water (25 mL), and basified with 50% aqueous NaOH. The products were extracted with ether (3 × 25 mL), and the combined ether extracts were washed with water (2 × 5 mL) and dried ($MgSO_4$). Evaporation of the ether gave a mixture of pale yellow liquid formate esters. Hydrolysis was achieved by dissolving the esters in ether (20 mL) and adding the ether solution dropwise to a stirred slurry of $LiAlH_4$ (150 mg, 4 mmol) in ether (20 mL). The mixture was heated at reflux for 1 h after complete addition, cooled, and quenched by adding it to 50 mL of a 1:1 mixture of water–10% aqueous H_2SO_4. The desired alcohol mixture was obtained by using ether extraction, and the alcohol mixture in acetone was oxidized to the corresponding ketones **1** and **2** by Jones reagent. Excess oxidant was decomposed by adding 2-propanol. The solution was diluted with ether (25 mL) and neutralized with 5% aqueous $NaHCO_3$. Solids were removed by filtration, the filtrate was extracted with ether, and the ether layer was dried ($MgSO_4$) to give a pale yellow solid. The solid was sublimed (110°, 1 at) to yield white crystals (515 mg, 83%) of a 1:1 mixture of **1** and **2** (GC, column A). The faster moving component of the mixture was separated by preparative GC on column E to give a 41% yield of >99% pure **1**, mp 187–189 °C (sealed capillary) [lit.[5a] mp 185–187 °C]; $[\alpha]^{25}_{589}$ +10.11°, $[\alpha]^{25}_{578}$ +10.62°, $[\alpha]^{25}_{436}$ +20.29°, $[\alpha]^{25}_{365}$ +30.15°, (*c* 0.68); UV (MI) $\epsilon_{290}{}^{max}$ = 17; UV (EPA) $\epsilon_{287}{}^{max}$ 21; CD (MI) $\Delta\epsilon_{250} = 0$, $\Delta\epsilon_{281.5} = +0.020$, $\Delta\epsilon_{291} = +0.022$, $\Delta\epsilon_{301} = +0.023$, $\Delta\epsilon_{312.5} = +0.025$, $\Delta\epsilon_{323.5} = +0.013$, $\Delta\epsilon_{339} = 0$; CD (EPA) $\Delta\epsilon_{272} = 0$, $\Delta\epsilon_{288} = -0.026$, $\Delta\epsilon_{296.5} = -0.045$, $\Delta\epsilon_{305.5} = -0.046$, $\Delta\epsilon_{316} = -0.019$, $\Delta\epsilon_{321} = 0$ (CD run at room temperature and data corrected to 100% e.e.); IR (CCl_4) 2920, 2860, 1715, 1065 cm^{-1}; ^1H NMR δ 0.95 (d, 3 H, *J* = 7 Hz, CH_3), 1.6–2.55 (br m, 13 H); ^{13}C NMR in Table I; MS, *m/z* (relative intensity) 164.1199 [$M^{+\cdot}$ $C_{11}H_{16}O$] (100), 149.0964 [$C_{10}H_{13}O$] (2), 146.1089 [$C_{11}H_{14}$] (2), 131.0859 [$C_{10}H_{11}$] (9), 121.1016 [C_9H_{13}] (13), 121.0653 [C_8H_9O] (8) amu.

(+)-(1*S*,3*R*)-4(*R*)(e)-Methyladamantan-2-one (2). The equatorial methyl epimer (**2**) formed and separated above by preparative GC had mp 165–167° (sealed capillary); $[\alpha]^{25}_{589}$ 0°, $[\alpha]^{25}_{578}$ 0°, $[\alpha]^{25}_{436}$ +11.9°, $[\alpha]^{25}_{365}$ +54.29° (c 0.97); UV (MI) $\epsilon_{293}{}^{max}$ 19; UV EPA $\Delta\epsilon_{290}{}^{max}$ = 22; CD (MI) $\Delta\epsilon_{252} = 0$, $\Delta\epsilon_{287} = +0.393$, $\Delta\epsilon_{295.5} = +0.479$, $\Delta\epsilon_{305} = +0.544$, $\Delta\epsilon_{316.5} = +0.362$, $\Delta\epsilon_{332} = 0$; CD (EPA) $\Delta\epsilon_{242} = 0$, $\Delta\epsilon_{294.5} = +0.671$, $\Delta\epsilon_{303} = +0.643$, $\Delta\epsilon_{310} = +0.306$, $\Delta\epsilon_{332} = 0$ (CD run at room temperature and data corrected to 100% e.e.); IR ($CHCl_3$) 2920, 2860, 1710, 1055 cm^{-1}; ^1H NMR δ 1.07 (d, 3 H, *J* = 7 Hz, CH_3), 1.4–2.47 (br m, 13 H) ppm; ^{13}C NMR in Table I; MS, *m/z* (relative intensity) 164.1199 [$M^{+\cdot}$ $C_{11}H_{16}O$] (100), 149.0968 [$C_{10}H_{13}O$] (3), 146.1092 [$C_{11}H_{14}$] (4), 131.0860 [$C_{10}H_{11}$] (15), 121.1017 [C_9H_{13}] (20), 121.0653 [C_8H_9O] (5) amu.

Enantiomeric Excess (e.e.) and Absolute Configuration of 1. The axial methyl ketone **1** obtained above (11 mg, 0.067 mmol) was reduced quantitatively and stereospecifically to the syn alcohol **26a + 26b** with $LiAlH_4$ in ether. Analytical GC (columns A and C) indicated only one epimer, which was derivatized as its Mosher ester[25] with (*R*)-(+)-α-methoxy-α-(trifluoromethyl)phenylacetic acid as previously described,[24] except 4-(dimethylamino)pyridine was added to facilitate esterification of this sterically hindered alcohol. In the ^1H NMR spectrum, the diastereomeric OCH_3 groups appeared as a single line (δ 5.20) that separated into two lines after addition of Eu(fod)$_3$ shift reagent (Aldrich), δ 6.67 and 6.55 in an integrated ratio of roughly 3:1 respectively. In the ^{19}F NMR spectrum run in $CDCl_3$ + $CFCl_3$ the diastereomeric CF_3 signals of the Mosher ester were split into two lines even without resorting to adding Eu(fod)$_3$, δ 35.12 and 34.92 ppm downfield from $CFCl_3$ internal standard in the ratio 1.000:3.253, respectively. Accordingly, alcohol **26a + 26b** has a 52.97 ± 2.0% e.e. of one enantiomer. This means that the parent ketone **1**, with $[\alpha]^{25}_{589}$ −10.11°, $[\alpha]^{25}_{365}$ −30.15° (*c* 0.68) and its parent, starting acid **15** have the same e.e.—in confirmation of the earlier findings.[21]

The absolute configuration of the predominant enantiomer is assigned 1*S*,3*R*, corresponding to **26a**, because the more intense resonances of the ^{19}F and ^1H NMR signals for the diastereomeric CF_3 and OCH_3 groups were faster moving upon addition of Eu(fod)$_3$.[25] The shifts were: 34.92 → 35.88 → 37.63 → 40.74 ppm for the more intense ^{19}F signal and 35.12 → 37.74 → 35.99 → 37.74 → 40.74 ppm for the less intense ^{19}F signal. Consistent with this conclusion, the ^{19}F NMR of the Mosher ester of alcohol **26b**, derived from the optically pure enantiomer (**27**) of **1**, which had been prepared by an independent route,[5a] showed only one resonance, δ 35.10, corresponding to the slower moving, less intense signal above. This means that the structures shown for **1** and **15** (and all other derivatives of **15**) represent the absolute configurations of the predominant enantiomers in this work. These findings independently confirm the absolute configurations determined previously by CD on 4,4-dimethyladamantan-2-one[21c] and 4-equatorial-substituted adamantan-2-ones.[36]

(36) Snatzke, G.; Eckhardt, G. *Chem. Ber.* **1968**, *101*, 2010–2027.

(+)-(1*R*,5*S*)-*endo*-(3(*R*)-Bicyclo[3.3.1]non-6-enyl) Ethyl Ketone (18). This ketone was prepared in essentially the same way as was the related methyl ketone **16**. Thus, an ethereal solution of ethyl lithium (0.493 M, 28 mL) was added to a vigorously stirred solution of (+)-(1*R*,5*S*)-*endo*-bicyclo[3.3.1]non-6-ene-3(*R*)-carboxylic acid (**15**) (1.0 g, 595 mmol), $[\alpha]^{25}_{578}$ +52.63° (*c* 0.9), 35.01% e.e., to afford 0.89 g (83%) of the colorless liquid ketone, bp 83–87° (2 mm). It was >99% pure by GC on column **B** and had $[\alpha]^{24}_{578}$ +35.5° (*c* 0.5); IR (neat) 3030, 2920, 1705, 1465, 920 cm^{-1}; ^1H NMR δ 0.93 (t, 3 H, *J* = 7 Hz), 1.60 (m, 2 H) 1.83–3.08 (br m, 11 H), 5.47 (br t, 2 H).

Anal. Calcd for $C_{12}H_{18}O$ (178): C, 80.85; H, 10.18. Found: C, 79.84; H, 10.04.

(+)-(1*R*,5*S*)-*endo*-3(*R*)-(Hydroxypropyl)bicyclo[3.3.1]non-6-ene (19). This alcohol was prepared by $LiAlH_4$ reduction of ketone **18** by the method used to reduce **16** to **17**. Thus, ketone **18** from above (0.6 g, 3.4 mmol $[\alpha]^{25}_{578}$ +35.50°, 35% e.e.) gave 0.44 g (72.5%) of colorless, oily alcohol **19** after distillation, bp 96–98 °C (2.5 mm). It was >99% pure by GC on column A and had $[\alpha]^{25}_{578}$ +81.1° (*c* 1.5), IR (neat) 3100–3000, 3030, 2930, 1455, 965 cm^{-1}; ^1H NMR δ 1.0 (t, 3 H, *J* = 6 Hz), 1.10–2.77 (br m, 13 H), 3.10–3.83 (br m 2 H).

Anal. Calcd for $C_{12}H_{20}O$ (180): C, 79.94; H, 11.18. Found: C, 79.98; H, 11.14.

(−)-(1*S*,3*R*)-4(*S*)(a)-Ethyladamantan-2-one (3). Alcohol **19** was cyclized in hot formic acid as described in synthesis of **1**, saponified, and oxidized to give a 1:1 mixture of axial (**3**) and equatorial (**4**) ethyladamantanones, as determined by GC on column C. Thus, alcohol **19** from above (0.30 g, 1.67 mmol, $[\alpha]^{25}_{578}$ +81.0) was converted to 183 mg of the oily ketonic mixture, which was separated by preparative GC on column E to afford >99% purity (GC, column C): 4(a)-ethyladamantanone (**3**) oil, 71 mg (24%) and 4(e)-ethyladamantanone (**4**) oil, 78 mg (26%). The axial ethylketone (**3**) had $[\alpha]^{22}_{365}$ −4.38° (*c* 0.12) for 35% e.e.; UV (MI) $\epsilon_{295}{}^{max}$ 17; UV (EPA) $\epsilon_{288}{}^{max}$ 22; CD (MI) $\Delta\epsilon_{250} = 0$, $\Delta\epsilon_{287} = -0.060$, $\Delta\epsilon_{296} = -0.088$, $\Delta\epsilon_{306.5} = -0.095$, $\Delta\epsilon_{318} = -0.036$, $\Delta\epsilon_{324} = 0$; CD (EPA) $\Delta\epsilon_{343} = 0$, $\Delta\epsilon_{316} = -0.071$, $\Delta\epsilon_{305} = -0.139$, $\Delta\epsilon_{296} = -0.145$, $\Delta\epsilon_{260} = 0$ (CD run at room temperature and data corrected to 100% e.e.); IR (neat) 2910, 1720, 1455, 1060 cm^{-1}; ^1H NMR δ 0.88 (t, 3 H, *J* = 7 Hz), 1.0–1.44 (m, 2 H), 1.80–2.04 (br m, 13 H), 2.43 (s, 1 H); ^{13}C NMR in Table I; MS, *m/z* (relative intensity) 178.1356 [$M^{+\cdot}$ $C_{12}H_{18}O$] (100), 163.1121 [$C_{11}H_{15}O$] (3), 160.1248 [$C_{12}H_{16}$] (6), 149.0958 [$C_{10}H_{13}O$] (20), 135.0805 [$C_9H_{11}O$] (18), 121.1015 [C_9H_{13}] (41) amu.

Anal. Calcd for $C_{12}H_{18}O$ (178): C, 80.85; H, 10.18. Found: C, 80.60; H, 10.17.

(±)-(1*S*,3*R*)-4(*R*)(e)-Ethyladamantan-2-one (4). The equatorial ethyl epimer (78 mg, 26%) was isolated by preparative GC as indicated above. It had $[\alpha]^{25}_{436}$ +8.95°, $[\alpha]^{25}_{365}$ +36.32° (*c* 0.2); UV (MI 4:1) $\epsilon_{295}{}^{max}$ 22; UV (EPA) $\epsilon_{292}{}^{max}$ 25; CD (MI) $\Delta\epsilon_{245} = 0$, $\Delta\epsilon_{287} = +0.528$, $\Delta\epsilon_{296} = +0.788$, $\Delta\epsilon_{305.5} = +0.914$, $\Delta\epsilon_{317} = +0.621$, $\Delta\epsilon_{337} = 0$; CD (EPA) $\Delta\epsilon_{328} = 0$, $\Delta\epsilon_{314} = +0.389$, $\Delta\epsilon_{303} = +0.788$, $\Delta\epsilon_{295} = +0.811$, $\Delta\epsilon_{245} = 0$ (CD run at room temperature and data corrected to 100% e.e.); IR (neat) 2910, 1715, 1455, 1063 cm^{-1}; ^1H NMR δ 0.90 (t, 3 H, *J* = 7 Hz), 1.4–1.76 (br m, 2 H), 1.76–2.20 (br m, 12 H) 2.38 (d, 2 H), ^{13}C NMR in Table I; MS, *m/z* (relative intensity) 178.1356 [$M^{+\cdot}$ $C_{12}H_{18}O$] (71), 163.1119 [$C_{11}H_{15}O$] (1), 160.1251 [$C_{12}H_{16}$] (36), 149.0970 [$C_{10}H_{13}O$] (26), 135.0888 [$C_9H_{12}O$] (1), 121.1016 [C_9H_{13}] (100) amu.

Anal. Calcd for $C_{12}H_{18}$ (178): C, 80.85; H, 10.18. Found: C, 80.97; H, 10.13.

(+)-(1*R*,5*S*)-*endo*-(3(*R*)-Bicyclo[3.3.1]non-6-enyl) Isopropyl Ketone (20). Isopropyl chloride (2.4 g, 30 mmol) was added dropwise (under an argon atmosphere) to a well-stirred suspension of finely powdered lithium (250 mg) in dry ether (50 mL) while maintaining the temperature of the mixture near −40 °C. After the addition was complete, the mixture was stirred for a period of 3 h at −40 °C. (+)-*endo*-Bicyclo-[3.3.1]non-6-ene-3(*R*)-carboxylic acid (**15**), (1.5 g, 9 mmol), $[\alpha]^{25}_{578}$ +55.02° (*c* 1.0), 36.60% e.e., dissolved in dry ether (50 mL) was then added dropwise under an argon atmosphere to the isopropyl lithium reagent mixture prepared above. After stirring the mixture for a period of 1 h at −40 °C, it was allowed to warm up to room temperature. Thereafter, the stirring was continued for 4 more h. The reaction was quenched and worked up as in the preparation of **16** (above) to yield 900 mg (52%) of a colorless semisolid following kugelrohr distillation, bp 102–105 °C (2.4 mm). It was >99% pure by GC on column A and had $[\alpha]^{25}_{589}$ +29.67° $[\alpha]^{25}_{578}$ +30.86°, (*c* 0.6); IR (neat) 3020, 2920, 1700, 1450, 1380, 1360, 1350 cm^{-1}; ^1H NMR δ 0.97 (d, *J* = 6 Hz, 6 H), 1.4–2.6 (br m, 11 H), 2.97 (heptet, 1 H, *J* = 6 Hz), 5.2–5.8 (br m, 2 H).

Anal. Calcd for $C_{13}H_{20}O$ (192): C, 81.20; H, 10.48. Found: C, 80.51; H, 10.22.

(+)-(1*R*,5*S*)-*endo*-3(*R*)-(1-Hydroxy-2-methylpropyl)bicyclo[3.3.1]-non-6-ene (21). A solution of ketone **20** (800 mg, 4.17 mmol), $[\alpha]^{25}_{589}$ +29.67° (*c* 0.6), 36.6% e.e., in dry ether (20 mL) was reduced exactly

as described in the preparation of **17** (above) to give 780 mg (96%) of a colorless oil following kugelrohr distillation, bp 123–126 °C (2.4 mm). It was >99% pure by GC on column A and had $[\alpha]^{25}_{589}$ +92.22° $[\alpha]^{25}_{578}$ +95.85°, (*c* 0.55); IR (neat) 3700–3100, 2930, 1385, 1365, 995 cm^{-1}; ^1H NMR 0.87 (d, 3 H, *J* = 6 Hz), 1.10–2.23 (br m, 12 H), 2.97–3.23 (m, 1 H), 3.23–3.67 (m, 1 H), 5.17–5.98 (br m, 2 H).

Anal. Calcd. for $C_{13}H_{22}O$ (194): C, 80.36; H, 11.41. Found: C, 80.24; H, 11.38.

(−)-(1*S*,3*R*)-4(*S*)(a)-Isopropyladamantan-2-one (5). Alcohol **21** (700 mg, 3.61 mmol), $[\alpha]^{25}_{589}$ +92.22° (*c* 0.55), 36.60% e.e. was cyclized in 20 mL of 88% formic acid and saponified as described for **1** (above) to afford a pale yellow liquid mixture of 4-isopropyladamantan-2-ols. The alcohols mixture was oxidized as described for **1** to give 500 mg of a 1:1 mixture (GC, column C) of axial (**5**) and equatorial (**6**) isopropyladamantanones. The mixture was separated by preparative GC on column E to give 190 mg (27%) of >99% pure faster moving axial isopropyl epimer **5** and 190 mg (27%) of >99% pure equatorial isopropyl epimer **6**. Axial epimer **5** had $[\alpha]^{25}_{589}$ −3.66°, $[\alpha]^{25}_{578}$ −3.84°, $[\alpha]^{25}_{436}$ −8.84°, $[\alpha]^{25}_{365}$ −18.28° (*c* 0.43) for 36.6% e.e.; UV (MI) ϵ_{290}^{max} 20; UV (EPA) ϵ_{292}^{max} 20; CD (MI) $\Delta\epsilon_{250} = 0$, $\Delta\epsilon_{287.5} = -0.109$, $\Delta\epsilon_{297} = -0.149$, $\Delta\epsilon_{306.5} = -0.142$, $\Delta\epsilon_{318} = -0.074$, $\Delta\epsilon_{330} = 0$; CD (EPA) $\Delta\epsilon_{330} = 0$, $\Delta\epsilon_{319} = -0.0713$, $\Delta\epsilon_{307} = -0.159$, $\Delta\epsilon_{297} = -0.172$, $\Delta\epsilon_{288} = -0.126$, $\Delta\epsilon_{255} = 0$ (CD run at room temperature and data corrected to 100% e.e.); IR (neat) 2930, 2860, 1725, 1480, 1460, 1390, 1370 cm^{-1}; ^1H NMR δ 0.83 (d, 3 H, *J* = 5.8 Hz), 0.94 (d, 3 H, *J* = 5.8 Hz), 1.45 (hept, 1 H, *J* = 6 Hz), 1.48–1.72 (br m, 1 H), 1.72–2.23 (br m, 10 H), 2.45 (br s, 1 H) 2.71 (br s, 1 H) ppm; ^{13}C NMR in Table I; MS, *m/z* (relative intensity) 192.1511 [$M^{+\cdot}$, $C_{13}H_{20}O$] (88), 177.1278 [$C_{12}H_{17}O$] (23), 174.1045 [$C_{13}H_{18}$] (7), 149.0961 [$C_{10}H_{13}O$] (64), 131.0857 [$C_{10}H_{11}$] (4), 121.1016 [C_9H_{13}] (100) amu.

Anal. Calcd for $C_{13}H_{20}O$ (192): C, 81.20; H, 10.48 Found: C, 81.18; H, 10.37.

(+)-(1*S*,3*R*)-4(e)-Isopropyladamantan-2-one (6). The equatorial isopropyl isomer **6** (190 mg, 27%) was isolated by preparative GC as indicated above (for **5**). It had $[\alpha]^{25}_{589}$ +2.66°, $[\alpha]^{25}_{578}$ +3.38°, $[\alpha]^{25}_{436}$ +12.66°, $[\alpha]^{25}_{365}$ = +44.63° (*c* 0.32); UV (MI) ϵ_{290}^{max} 22; UV (EPA) ϵ_{290}^{max} 27; CD (MI) $\Delta\epsilon_{250} = 0$, $\Delta\epsilon_{287} = +0.329$, $\Delta\epsilon_{296} = +0.503$, $\Delta\epsilon_{305.5} = +0.599$, $\Delta\epsilon_{317} = +0.412$, $\Delta\epsilon_{335} = 0$; CD (EPA) $\Delta\epsilon_{328} = 0$, $\Delta\epsilon_{315} = +0.393$, $\Delta\epsilon_{304} = +0.781$, $\Delta\epsilon_{295} = +0.798$, $\Delta\epsilon_{250} = 0$ (CD run at room temperature and data corrected to 100% e.e.); IR (neat) 2930, 2870, 1720, 1480, 1460, 1390, 1370 cm^{-1}; ^1H NMR, δ 0.88 (d, 3 H, *J* = 6.1), 0.94 (d, 3 H, *J* = 6.0), 1.2–1.48 (br m, 1 H), 1.48–2.32 (br m, 11 H), 2.4–2.72 (2 H, br s); ^{13}C NMR in Table I; MS, *m/z* (relative intensity) 192.1511 [$M^{+\cdot}$, $C_{13}H_{20}O$] (28), 177.1278 [$C_{12}H_{17}O$] (1), 174.1404 [$C_{13}H_{18}$] (6), 149.0969 [$C_{10}H_{13}O$] (55), 131.0860 [$C_{10}H_{11}$] (2), 121.1017 [C_9H_{13}] (100) amu.

Anal. Calcd for $C_{13}H_{20}O$ (192): C, 81.20; H, 10.48. Found: C, 81.01; H, 10.35.

(+)-(1*R*,5*S*)-*endo*-3(*R*)-Bicyclo[3.3.1]non-6-enyl *tert*-Butyl Ketone (22). A solution of *tert*-butyllithium in pentane (1.5 M, 9.1 mL, 13.6 mmol) was added dropwise to a well-stirred solution of (+)-**15** (1.0 g, 6.02 mmol), $[\alpha]^{25}_{578}$ +75.03° (*c* 1.0), 49.93% e.e., in pentane (75 mL). The mixture was stirred and heated at reflux for 7 h. The mixture was quenched following cooling by adding it to 50 mL of saturated aqueous NH_4Cl. The pentane layer was separated, and the aqueous layer was extracted with ether (3 × 25 mL). The combined organic layers were washed with water (20 mL), saturated aqueous $NaHCO_3$ (20 mL), and saturated aqueous NaCl (20 mL), and then dried ($MgSO_4$). The solvent was evaporated under reduced pressure, and the resultant yellow oil was partially purified by kugelrohr distillation, bp 112–116 °C (2.0 mm), to give 0.31 g (24%). An analytically pure sample (GC, column A) was prepared by preparative GC (column D). It had $[\alpha]^{25}_{589}$ +57.50°, $[\alpha]^{25}_{578}$ +61.25° (*c* 0.10); IR (neat) 3020, 3000–2800, 1705, 1400, 1370 cm^{-1}; ^1H NMR δ 1.12 (s, 3 H), 1.13 (s, 3 H), 1.14 (s, 3 H), 1.2–1.8 (br m, 7 H), 2.0–2.6 (br m, 4 H), 5.04–6.02 (br m, 2 H).

Anal. Calcd for $C_{14}H_{22}O$ (206): C, 81.50; H, 10.75. Found: C, 81.19; H, 10.82.

(+)-(1*R*,5*S*)-*endo*-3(*R*)-(1-Hydroxy-2,2-dimethylpropyl)bicyclo-[3.3.1]non-6-ene (23). A solution of ketone **22** (250 mg, 1.2 mmol), $[\alpha]^{25}_{589}$ +57.50° (*c* 0.10), 49.93% e.e., in dry ether (20 mL) was reduced exactly as described in the preparation of **17** (above) to give 230 mg (93%) of a colorless oil following kugelrohr distillation, bp 135–140 °C (2.5 mm). An analytically pure (>99%, GC, column A) was obtained by prep GC (column D) and had $[\alpha]^{25}_{578}$ +150.29°, $[\alpha]^{25}_{589}$ +144.26° (*c* 0.17); IR (neat) 3600–3500, 3020, 3000–2800, 1395–1365 cm^{-1}; ^1H NMR δ 1.15 (s, 6 H), 1.20 (s, 3 H), 1.26 (s, 1 H), 1.28–1.9 (br m, 10 H), 2.0–2.5 (br m, 2 H), 5.4–6.0 (br m, 2 H).

Anal. Calcd for $C_{14}H_{24}O$ (208): C, 80.71; H, 11.61. Found: C, 80.45; H, 11.25.

(−)-(1*S*,3*R*)-4(*S*)(a)-*tert*-Butyladamantan-2-one (7). Alcohol **23** (0.20 g, 0.96 mmol), $[\alpha]^{25}_{589}$ +144.26° (*c* 0.17), 49.93% e.e., was cyclized in 6 mL of hot 88% formic acid as described for **1** (above) to afford a pale yellow oily mixture. The alcohol mixture was oxidized as described for **1** to give 160 mg of a viscous oily mixture of axial (**7**) and equatorial (**8**) *tert*-butyladamantanones and isopropylmethyladamantanones (**11** and **12**). Analytical GC (column A) indicated a 2:1 mixture of **7**:**8**, a 1:1 mixture of **11**:**12**, and a 1:4 mixture of (**7** + **8**):(**11** + **12**). The **11** + **12** pair is faster moving than the **7** + **8** pair. The mixture was separated by preparative GC (column D) to give 18 mg of **7** (9%), 8 mg of **8** (4%), 50 mg of **11** (25%) and 50 mg of **12** (25%), all of which were >99% pure. Axial *tert*-butyladamantanone **7** had $[\alpha]^{25}_{589}$ −12.0°, $[\alpha]^{25}_{578}$ −12.6°, $[\alpha]^{25}_{546}$ −14.2°, $[\alpha]^{25}_{436}$ −27.74°, $[\alpha]^{25}_{365}$ −60.65° (*c* 0.23) for 49.93% e.e; UV (MI) ϵ_{290}^{max} 25; UV (EPA) ϵ_{288}^{max} 27; CD (MI) $\Delta\epsilon_{252} = 0$,$\Delta\epsilon_{278} = -0.223$, $\Delta\epsilon_{296} = -0.293$, $\Delta\epsilon_{306} = -0.276$, $\Delta\epsilon_{317} = -0.144$, $\Delta\epsilon_{331} = 0$; CD (EPA) $\Delta\epsilon_{252} = 0$, $\Delta\epsilon_{296} = -0.535$, $\Delta\epsilon_{304} = -0.483$, $\Delta\epsilon_{315} = -0.262$, $\Delta\epsilon_{330} = 0$ (CD run at room temperature and corrected to 100% e.e.); IR (neat) 3000–2800, 1720, 1395, 1365 cm^{-1}; ^1H NMR δ 0.92 (s, 9 H), 1.55 (br s, 1 H), 2.0 (br m, 2 H), 2.26 (br s, 2 H), 2.49 (br s, 2 H), 2.78 (br s, 2 H) ppm; ^{13}C NMR in Table I; MS, *m/z* (relative intensity) 206.1668 [$M^{+\cdot}$ $C_{14}H_{22}O$] (13), 150.1040 [$C_{10}H_{14}O$] (100), 149.1326 [$C_{10}H_{13}O$] (6), 121.1019 [C_9H_{13}] (24) amu.

Anal. Calcd for $C_{14}H_{22}O$ (206): C, 81.50; H, 10.75. Found: C, 81.66; H, 11.01.

(+)-(1*S*,3*R*)-4(*R*)(e)-*tert*-Butyladamantan-2-one (8). The equatorial *tert*-butyl isomer (**8**) (8 mg, 4%) was isolated by preparative GC as indicated above (for **7**). It had $[\alpha]^{25}_{589}$ +13.27°, $[\alpha]^{25}_{578}$ +16.92°, $[\alpha]^{25}_{546}$ +17.70°, $[\alpha]^{25}_{436}$ +34.42°, $[\alpha]^{25}_{365}$ +85.00° (*c* 0.13); UV (MI) ϵ_{288}^{max} 26; UV (EPA) ϵ_{284}^{max} 27; CD (MI) $\Delta\epsilon_{250} = 0$, $\Delta\epsilon_{295} = +0.670$, $\Delta\epsilon_{304} = +0.753$, $\Delta\epsilon_{315} = +0.505$, $\Delta\epsilon_{336} = 0$; CD (EPA) $\Delta\epsilon_{250} = 0$, $\Delta\epsilon_{295} = +0.774$, $\Delta\epsilon_{303} = +0.743$, $\Delta\epsilon_{315} = +0.355$, $\Delta\epsilon_{336} = 0$ (CD run at room temperature and corrected to 100% e.e.); IR (neat) 3000–2800, 1720, 1395, 1365 cm^{-1}; ^1H NMR δ 1.04 (s, 9 H), 1.26 (br s, 1 H), 1.53 (br s, 2 H), 1.7 (br s 2 H), 1.97 (br m, 2 H), 2.23 (br m, 2 H), 2.75 (br s, 2 H); ^{13}C NMR in Table I; MS, *m/z* (relative intensity) 206.1669 [$M^{+\cdot}$ $C_{14}H_{22}O$] (19), 150.1030 [$C_{10}H_{14}O$] (16), 149.0967 [$C_{10}H_{13}O$] (72), 121.1017 [C_9H_{13}] (100) amu.

Anal. Calcd for $C_{14}H_{22}O$ (206): C, 81.50; H, 10.75. Found: C, 81.33; H, 10.95.

(+)-(1*S*,3*R*)-4(*S*)(a)-Isopropyl-4(*R*)(e)-methyladamantan-2-one (11). The rearranged isomer, **11** (50 mg, 25%) was isolated by preparative GC as indicated above (for **7**). It had $[\alpha]^{25}_{589}$ +11.50°, $[\alpha]^{25}_{578}$ +12.10°, $[\alpha]^{25}_{546}$ +14.04, $[\alpha]^{25}_{436}$ +31.66°, $[\alpha]^{25}_{365}$ +83.75° (*c* 0.14) for 49.93% e.e.; UV (MI) ϵ_{295}^{max} 20; UV (EPA) ϵ_{285}^{max} 24; CD (MI) $\Delta\epsilon_{250} = 0$, $\Delta\epsilon_{296} = +0.705$, $\Delta\epsilon_{305} = +0.819$, $\Delta\epsilon_{316} = +0.552$, $\Delta\epsilon_{340} = 0$; CD (EPA) $\Delta\epsilon_{248} = 0$, $\Delta\epsilon_{295} = +0.693$, $\Delta\epsilon_{303} = +0.668$, $\Delta\epsilon_{313} = +0.396$, $\Delta\epsilon_{344} = 0$ (CD run at room temperature and corrected to 100% e.e.); IR (neat) 3000–2860, 1710, 1390–1370 cm^{-1}; ^1H NMR δ 0.745 (d, 3 H, *J* = 6.6 Hz), 0.835 (d, 3 H, *J* = 6.8 Hz), 0.94 (s, 3 H), 1.26 (m, 1 H), 1.5–2.4 (br m, 12 H) ppm; ^{13}C NMR in Table I; MS, *m/z* (relative intensity) 206.1669 [$C_{14}H_{22}O$] (18), 191.1432 [$C_{13}H_{19}O$] (1), 163.1120 [$C_{11}H_{15}O$] (83), 135.1167 [$C_{10}H_{15}$] (100) amu.

Anal. Calcd for $C_{14}H_{22}O$ (206): C, 81.50; H, 10.75. Found: C, 81.42; H, 10.99.

(+)-(1*S*,3*R*)-4(*R*)(e)-Isopropyl-4(*S*)(a)-methyladamantan-2-one (12). The rearranged isomer, **12** (50 mg, 25%) was isolated by preparative GC as indicated above (for **7**). It had $[\alpha]^{25}_{589}$ +14.46°, $[\alpha]^{25}_{578}$ +14.93°, $[\alpha]^{25}_{546}$ +17.09°, $[\alpha]^{25}_{436}$ +37.84°, $[\alpha]^{25}_{365}$ 89.51° (*c* 0.37); UV (MI) ϵ_{290}^{max} = 23; UV (EPA) ϵ_{286}^{max} = 25; CD (MI) $\Delta\epsilon_{250} = 0$, $\Delta\epsilon_{296} = +0.647$, $\Delta\epsilon_{306} = +0.724$, $\Delta\epsilon_{318} = +0.476$, $\Delta\epsilon_{335} = 0$; CD (EPA) $\Delta\epsilon_{251} = 0$, $\Delta\epsilon_{295} = +0.551$, $\Delta\epsilon_{304} = +0.518$, $\Delta\epsilon_{313} = +0.259$, $\Delta\epsilon_{327} = 0$ (CD run at room temperature and corrected to 100% e.e.); IR (neat) 3000–2820, 1710, 1390, 1370, 1365 cm^{-1}; ^1H NMR δ 0.703 (s, 3 H), 0.766 (d, *J* = 6.8 Hz, 3 H), 0.831 (d, *J* = 6.1, 3 H), 1.15 (m, 1 H), 1.6–2.4 (br m, 12 H) ppm; ^{13}C NMR in Table I; MS, *m/z* (relative intensity) 206.1668 [$C_{14}H_{22}O$] (13), 191.1432 [$C_{13}H_{19}O$] (0.3), 163.1121 [$C_{11}H_{15}O$] (84), 135.1168 [$C_{10}H_{15}$] (100) amu.

Anal. Calcd for $C_{14}H_{22}O$ (206): C, 81.50; H, 10.75. Found: C, 81.57; H, 10.59.

(+)-(1*R*,5*S*)-*endo*-3(*R*)-Bicyclo[3.3.1]non-6-enyl 3,3-Dimethylbutyl Ketone (24). A solution of *tert*-butyllithium in pentane (Alfa) (1.9 *M*, 14.3 mL, 27.2 mmol) was added slowly (Ar atmosphere) to a vigorously stirred solution of (+)-**15** (2.0 g, 12.05 mmol), $[\alpha]^{25}_{578}$ +79.83° (*c* 1.2), 53.31% e.e. in dry ether (50 mL). The reaction was carried out as described above for **16** to give 820 mg crude yield of a yellow semisolid found to have three components by GC on column A. The major component, **24**, was isolated by column chromatography on silica gel (J. T. Baker) using hexane–ether (5:1) as a colorless liquid, 490 mg (20%). It was >99% pure by GC on column A and had $[\alpha]^{25}_{589}$ +52.09°, $[\alpha]^{25}_{578}$ +54.78° (*c* 0.46); IR (neat) 3040, 2950, 1715, 1475, 1370 cm^{-1}; ^1H

NMR δ 0.88 (s, 9 H), 0.98 (s, 2 H), 1.24 (br s, 4 H), 1.4–2.2 (br m, 9 H), 5.4–5.9 (br m, 2 H).

Anal. Calcd for $C_{16}H_{26}O$ (234): C, 81.99; H, 11.18. Found: C, 82.09; H, 10.86.

(+)-(1*R*,5*S*)-*endo*-3(*R*)-(1-Hydroxy-4,4-dimethylhexyl)bicyclo-[3.3.1]non-6-ene (25). Four hundred and fifty milligrams (2.18 mmol) of ketone **24** from above, $[\alpha]^{25}_{578}$ +54.78° (c 0.46), 53.13% e.e. was reduced with $LiAlH_4$ as described for **17** (above) to give 420 mg (93%) of oily alcohol **25**. It had $[\alpha]^{25}_{598}$ +75.45°, $[\alpha]^{25}_{578}$ +80.91° (*c* 0.11); IR (neat) 3680–3080, 3010, 2920, 1460, 1360 cm^{-1}; ^1H NMR δ 0.86 (9 H, s), 1.02 (br s, 2 H), 2.0–2.28 (br m, 6 H), 5.4–5.8 (br m, 2 H).

Anal. Calcd. for $C_{16}H_{28}O$ (236): C, 81.29; H, 11.94. Found: C, 81.48; H, 10.53.

(−)-(1*S*,3*R*)-4(*S*)(a)-(3,3-dimethylbutyl)adamantan-2-one (9). Alcohol **25** (400 mg, 1.92 mmol), $[\alpha]^{25}_{578}$ +80.91° (*c* 0.1), 53.13% e.e. was cyclized in hot formic acid as described in the synthesis of **1**. The formate esters were cleaned with $LiAlH_4$, and the resultant alcohol mixture was oxidized with 1.5 equiv of pyridinium chlorochromate to give 240 mg of a crude mixture (1:1, by GC on column C) of ketones **9** and **10**. The liquid ketones were separated and purified by preparative GC on column E to give 110 mg (27%) of >99% pure faster moving axial epimer **9** and 110 mg (27%) of pure equatorial epimer **10**. Axial ketone **9** had $[\alpha]^{25}_{589}$ ~0°, $[\alpha]^{25}_{578}$ ~0°, $[\alpha]^{25}_{436}$ ~0, $[\alpha]^{25}_{365}$ −5.15° (*c* 0.51) for 53.1% of e.e.; UV (MI) ϵ_{289}^{max} 18; UV (EPA) ϵ_{286}^{max} 21.3; CD (MI) $\Delta\epsilon_{252}$ = 0, $\Delta\epsilon_{288}$ = −0.079, $\Delta\epsilon_{296.5}$ = −0.100, $\Delta\epsilon_{306.5}$ = −0.093, $\Delta\epsilon_{317}$ = −0.057, $\Delta\epsilon_{348}$ = 0; CD (EPA) $\Delta\epsilon_{348}$ = 0, $\Delta\epsilon_{316}$ = −0.082, $\Delta\epsilon_{305}$ = −0.16, $\Delta\epsilon_{296}$ = −0.174, $\Delta\epsilon_{287}$ = −0.135, $\Delta\epsilon_{249}$ = 0 (CD run at room temperature and corrected to 100% e.e.); IR (neat) 2940, 2870, 1730, 1475, 1370 cm^{-1}; ^1H NMR δ 0.84 (s, 9 H), 1.08 (br m, 4 H), 1.6–2.2 (br m, 11 H), 2.40 (br s, 2 H); ^{13}C NMR in Table I; MS, *m/z* (relative intensity) 234.1984 [M^{+} $C_{16}H_{26}O$] (49), 219.1748 [$C_{15}H_{23}O$] (24), 216.1882 [$C_{16}H_{24}$] (1), 201.1650 [$C_{15}H_{21}$] (26), 191.1438 [$C_{13}H_{19}O$] (7), 178.1352 [$C_{12}H_{18}O$] (52), 177.1279 [$C_{12}H_{17}O$], (57), 163.1124 [$C_{11}H_{15}O$] (11), 160.1252 [$C_{12}H_{16}$] (18), 150.1032 [$C_{10}H_{14}O$] (10), 149.1329 [$C_{11}H_{17}$] (11), 149.0967 [$C_{10}H_{13}O$] (28), 135.0814 [$C_9H_{11}O$] (11), 121.1019 [C_9H_{13}] (32), 57.0624 (C_4H_9] (100) amu.

Anal. Calcd. for $C_{16}H_{26}O$ (234): C, 81.99; H, 11.18. Found: C, 80.72; H, 10.62.

(+)-(1*S*,3*R*)-4(*R*)(e)-(3,3-dimethylbutyl)adamantan-2-one (10). The equatorial isomer **10** (110 mg, 27%) was isolated by preparative GC as indicated above (for **9**). It had $[\alpha]^{25}_{589}$ +8.57°, $[\alpha]^{25}_{578}$ +9.05°, $[\alpha]_{546}$ +10.48°, $[\alpha]^{25}_{436}$ +19.52°, $[\alpha]^{25}_{365}$ +53.80°, (*c* 0.21); UV (MI) ϵ_{285}^{max} 22; UV (EPA) ϵ_{285}^{max} 29.5; CD (MI) $\Delta\epsilon_{244}$ = 0, $\Delta\epsilon_{287}$ = +0.414, $\Delta\epsilon_{296}$ = +0.605, $\Delta\epsilon_{305.5}$ = +0.685, $\Delta\epsilon_{316.5}$ = +0.454, $\Delta\epsilon_{334}$ = 0; CD (EPA) $\Delta\epsilon_{333}$ = +0.443, $\Delta\epsilon_{304}$ = 0.902, $\Delta\epsilon_{295}$ = 0.923, $\Delta\epsilon_{241}$ = 0 (CD run at room temperature and corrected to 100% e.e.); IR (neat) 2940, 2870, 1720, 1480, 1370 cm^{-1}; ^1H NMR δ 0.84 (s, 9 H), 0.9–1.2 (br m, 4 H), 2.2–2.6 (br d, 2 H); ^{13}C NMR in Table I; MS, *m/z* (relative intensity) 234.1986 [M^{+} $C_{16}H_{26}O$] (46), 219.1748 [$C_{15}H_{23}O$] (3), 216.1878 [$C_{16}H_{24}$] (3), 201.1648 [$C_{15}H_{21}$] (15), 191.1442 [$C_{13}H_{19}O$] (0.7), 178.1358 [$C_{12}H_{18}O$] (48), 177.1283 [$C_{12}H_{17}O$], (9), 163.1123 [$C_{11}H_{15}O$] (3), 160.1252 [$C_{12}H_{16}$] (16), 150.1039 [$C_{10}H_{14}O$] (28), 149.1130 [$C_{11}H_{17}$] (6), 149.0968 [$C_{10}H_{13}O$] (34), 135.0815 [$C_9H_{11}O$] (4), 121.1016 [C_9H_{13}] (100) amu.

Anal. Calcd. for $C_{16}H_{26}O$ (234): C, 81.99; H, 11.18. Found: C, 81.71; H, 11.06.

(+)-(1*R*,3*S*)-4(*R*)(a)-Deuterioadamantan-2-one (13). This chiral deuterio ketone was prepared by a modification of the procedure of Numan and Wynberg.[21b] Thus, (+)-*endo*-bicyclo[3.3.1]non-6-ene-3-carboxylic acid (**15**), 1.0 g, 5.95 mmol, $[\alpha]^{25}_{578}$ +112.4° (*c* 0.25), 75% e.e., was cyclized in acetic anhydride–boron trifluoride etherate in dry benzene at room temperature and hydrolyzed as described,[21b] to yield 0.81 g (81%) of an epimeric mixture of (1*R*,3*S*)-4(*R*)(a)-hydroxyadamantan-2-one and (1*R*,3*S*)-4(*S*)(e)-hydroxyadamantan-2-one. The mixture was ketalized with ethylene glycol/*p*-toluenesulfonic acid[21b] and oxidized with pyridinium chlorochromate to give a 48% yield of (−)-(1*S*,3*S*)-4-ethylenedioxyadamantan-2-one, $[\alpha]^{25}_{578}$ −18.62° (*c* 0.9), 75% e.e. This material was reduced with $LiAlD_4$ (Stohler, 99%D) in ether and deketalized to afford (1*R*,3*S*)-4(e)-deuterio-4(*R*)(a)-hydroxyadamantan-2-one which was converted in 82% yield to its methanesulfonate with methanesulfonyl chloride/triethylamine in CH_2Cl_2. Treatment of the methanesulfonate with $LiAlH_4$ in ether, followed by pyridinium chlorochromate oxidation gave ketone **13** in 71% yield. It was sublimed and had mp 252–255 °C; $[\alpha]^{25}_{578}$ = +1.66° (*c* 0.25, isopentane); UV (MI) ϵ_{293}^{max} 18; UV (EPA) ϵ_{287}^{max} 23; CD (MI 4:1) $\Delta\epsilon_{275}$ = 0; $\Delta\epsilon_{286}$ = +0.008, $\Delta\epsilon_{292}$ = +0.014, $\Delta\epsilon_{296}$ = +0.016, $\Delta\epsilon_{302}$ = +0.014, $\Delta\epsilon_{307}$ = +0.014, $\Delta\epsilon_{313}$ = +0.01, $\Delta\epsilon_{350}$ = 0; CD (EPA) $\Delta\epsilon_{275}$ = 0, $\Delta\epsilon_{286}$ = +0.008, $\Delta\epsilon_{291}$ = +0.009, $\Delta\epsilon_{295}$ = +0.01, $\Delta\epsilon_{301}$ = +0.008, $\Delta\epsilon_{306}$ = +0.007, $\Delta\epsilon_{312}$ = +0.004, $\Delta\epsilon_{320}$ = 0 (CD run at room temperature and corrected to 100% e.e. and 100% d_1); IR ($CHCl_3$) 2930, 2160, 2000, 1720, 1700, 1450 cm^{-1}; ^1H NMR δ 1.75–2.25 (br m, 11 H), 2.4–2.65 (m, 2 H); ^{13}C NMR in Table I; MS, *m/z* (relative intensity) 151.1103 [M^{+}, calcd for $C_{10}H_{13}DO$, 151.1107] (100) amu.

(+)-(1*R*,3*S*)-4(*S*)(e)-Deuterioadamantan-2-one (14). The equatorial deuterio ketone was prepared by a modification of the procedure of Numan and Wynberg[21b] as described above, except the (−)-(1*R*,3*S*)-4-ethylenedioxyadamantan-2-one used above, $[\alpha]^{25}_{578}$ −18.62° (*c* 0.9), 75% e.e., was reduced with $LiAlH_4$ instead of $LiAlD_4$ and the resulting hydroxyketone, derivatized as its methanesulfonate, was treated with $LiAlD_4$ to produce ketone **14** in 63% yield after sublimation. It had mp 253–256 °C; $[\alpha]^{22}_{578}$ +2.58 (*c* 0.3, isopentane); UV (MI) ϵ_{293}^{max} = 18; UV (EPA) ϵ_{283}^{max} = 21; CD (MI) $\Delta\epsilon_{260}$ = 0, $\Delta\epsilon_{279}$ = +0.05, $\Delta\epsilon_{287}$ = +0.087, $\Delta\epsilon_{296}$ = +0.12, $\Delta\epsilon_{306}$ = +0.11, $\Delta\epsilon_{317}$ = +0.069, $\Delta\epsilon_{347}$ = 0; CD (EPA) $\Delta\epsilon_{257}$ = 0, $\Delta\epsilon_{286}$ = +0.084, $\Delta\epsilon_{295}$ = +0.11, $\Delta\epsilon_{305}$ = +0.09, $\Delta\epsilon_{315}$ = +0.05, $\Delta\epsilon_{326}$ = 0 (CD run at room temperature and corrected to 100% e.e. and 100% d_1); IR ($CHCl_3$) 2925, 2160, 1720, 1700, 1460, 1060 cm^{-1}; ^1H NMR δ 1.88–2.3 (br m, 11 H), 2.4–2.6 (m, 2 H); ^{13}C NMR in Table I; MS, *m/z* (relative intensity) 151.1102 [M^{+}, calcd for $C_{10}H_{13}DO$, 151.1107] (100) amu.

Acknowledgment. We thank the National Science Foundation (CHE 8218216) for generous support of this work. We thank also J. W. Givens III and Dr. S. L. Rodgers for assistance in the MM2 calculations.